Robust Stability Analysis for Class of Takagi-Sugeno (T-S) Fuzzy With Stochastic Process for Sustainable Hypersonic Vehicles

Muhammad Shamrooz Aslam[†‡] **Prayag Tiwari** [§*] **Hari Mohan Pandey** [¶*] **Shahab S. Band** [‖*]

Abstract

Recently, the rapid development of *Unmanned Aerial Vehicles (UAVs)* enables ecological conservation, such as low-carbon and "green" transport, which helps environmental sustainability. In order to address control issues in a given region, *UAV* charging infrastructure is urgently needed. To better achieve this task, an investigation into the T–S fuzzy modeling for *Sustainable Hypersonic Vehicles (SHVs)* with Markovian jump parameters and H_∞ attitude control in three channels was conducted. Initially, the reentry dynamics were transformed into a control–oriented affine nonlinear model. Then, the original T–S local modeling method for *SHV* was projected by primarily referring to *Taylor's expansion* and fuzzy linearization methodologies. After the estimation of precision and controller complexity was assumed, the fuzzy model for jump nonlinear systems mainly consisted of two levels: a crisp level and a fuzzy level. The former illustrates the jumps, and the latter a fuzzy level that represents the nonlinearities of the system. Then, a systematic method built in a new *coupled Lyapunov function* for a stochastic fuzzy controller was used to guarantee the closed–loop system for H_∞ gain in the presence of a predefined performance index. Ultimately, numerical simulations were conducted to show how the suggested controller can be successfully applied and functioned in controlling the original attitude dynamics.

Keywords: Stochastic system; H_∞ Control; Linear matrix inequalities; Stabilizing controller.

1 Introduction

With the growing demand and emerging technologies, there has been increasing popularity of electric vehicles and *UAVs*. In tandem with this trend, sustainability concerns have become more prominent in recent years. Adapting battery technology to electric vehicles has enabled them to help solve a number of pressing environmental issues, such as fossil fuel depletion [1]. Testing robust control methods on *UAVs* can be possibly challenging. Positioning performance needs to be fast, precise, and robust. Due to wireless transmission, position and linear velocity measurements during an indoor flight tend to occur. A delay is introduced into variables associated with the position of the vehicle in relation to the target by the image processing used in visual serving schemes. Aerodynamic changes during close–range flight complicate the common methods for controlling flying patterns. In comparison to traditional aircraft and ballistic vehicles, several nations around the world are investing time and money in developing *Sustainable hypersonic vehicles (SHVs)*. The purpose of doing so is to think highly of the advantages of their notable features of the extended flying range, excellent maneuverability, and powerful penetration via hypersonic glide in the

*Corresponding author. *Email addresses:* H.M. Pandey, P. Tiwari, S.S. Band.

†Artificial Intelligence Research Institute, China University of Mining and Technology, Xuzhou, China.
Email addresses: shamroz_aslam@yahoo.com (M.S. Aslam)

‡School of Automation, Guangxi University of Science and Technology, Liuzhou 545006, China.

§School of Information Technology, Halmstad University, Sweden. (email: prayag.tiwari@ieee.org)

¶Data Science & Artificial Intelligence Department, Bournemouth University, Fern Barrow, Poole, Dorset, BH12 5BB, UK.
Email addresses: hpandey@bournemouth.ac.uk

‖Future Technology Research Center, College of Future, National Yunlin University of Science and Technology, 123 University Road, Section 3, Douliou, Yunlin 64002, Taiwan, ROC. (email: shahab@yuntech.edu.tw)

upper atmosphere [2]. *SHVs*, referred to as a type of aerial vehicle, can glide over long distances at high speeds using aerodynamic forces. This is because an *SHV* travels near space, and the parameters of its operating environment are complicated. Moreover, the atmosphere's density could varies drastically with altitude. As a result, the aerodynamic loads tend to rapidly, and hence poses significant uncertainty. On the other hand, the T–S fuzzy method can be used to deal with uncertain nonlinear systems, which is a difficult problem, especially in terms of model accuracy. For this reason, fuzzy method has been developed and applied to the field of control theory. *Hyper–vehicles* are complex, and so nonlinear models cannot be controlled by traditional aircraft control methods due to their strong coupling, high nonlinearity, and uncertainty. As of date, many research studies have been conducted by numerous scholars to examine this problem. With the focus of the study placed on the different kinds of unknown disturbances. In [3], authors introduced *T-S fuzzy models* to describe disturbances in the longitudinal models of hypersonic flight vehicles and hence designed a disturbance observer–based controller to achieve better robust tracking performance. In [4], the authors constructed an *interval type–2 T–S fuzzy model* for analysis, and discussions on a controller with elevator faults are provided. In [5], a probabilistic robust fuzzy state feedback controller, which meets the required H_2/H_∞ performance, was designed by considering the uncertain parameters as normally distributed variables. In [6], a novel sliding mode learning control method, based on the concept of extended state observer, was introduced for hypersonic vehicles. This method is described as a *T–S fuzzy system*. According to the aforementioned study, the researchers focused on traditional disturbances. So it is necessary to handle the nonlinear terms by means of a stochastic process based upon a *T-S fuzzy system*. One of the goals of this paper is to approach nonlinear terms in a positive way. Therefore, numerous researchers have based their studies based on fuzzy control schemes [7] and predictive control design for mechanical systems [8]. Further, no single linear control scheme, even a nonlinear control scheme, can deal with these situations effectively. These features further highlight the importance of an efficient nonlinear control method as a fundamental process. However, numerous nonlinear control techniques have been refined and applied to research studies on the hypersonic vehicles [9].

In the past decades, it has been extensively studied how state-space linear systems with parameter uncertainty can exhibit robust stability, e.g., in power systems [10, 11], mechanical applications [12, 13], *UAV* systems [14], and robotic engineering applications [15, 16]. Moreover, novel criteria have been designed in [10] in order to improve the performance of the *Dynamic Voltage Restorer (DVR)*, while in [11], photovoltaic systems based on a grid–tie have been investigated for robust control. In the same consequence, an active suspension plant with a *sliding mode controller (SMC)* and unicycle for the quadratic stability analysis has been developed in [12, 13], respectively. Experimental level angular and translational positions for the *unmanned aircraft vehicle (UAV)* have been ensured with fast integral *SMC* [14], and simultaneously, authors have explored the optimal configuration of the robotic arm to reduce chattering behaviour in [15]. However, robust stability control and robustness have not been fully investigated in terms of *fuzzy Markov process systems*. The present study is motivated by this research gap in *fuzzy Markov process systems*, especially those containing complex coupling relationships between nonlinear terms.

This model for nonlinear plant dynamics is a major element of most model-based control techniques. However, due to the complexity of physical systems, obtaining a detailed mathematical model of a nonlinear system will be challenging. In integrating numerous local linear systems with non-linear membership functions, the *fuzzy-model-based (FMB)* method shall be employed in approximate non-linear systems [17]. In recent decades, fuzzy control systems, particularly *Takagi–Sugeno (T–S)* fuzzy model system, have gained a lot of interest from both theoretical and practical research [18], and hence some results generated from engineering applications, e.g., (hydro–turbine, cyber–security systems, maglev vehicles, electro-magnetic systems, servo–motors, manufacturing and production plant) have been obtained [19]. The T–S fuzzy approach can be clearly distinguished if used for a linear system model with flexible fuzzy linguistic theory to better define the local dynamics of each fuzzy rule. Now, to evaluate each linear model, one of the several linear control approaches can also be used. In the same context, the authors of [20] explored the issue of trajectory error with the variable bank angle and attack angle. This was in place of the nominal reverse logic of bank angle and angle of attack. So, the aim of this article is to provide the desired response to the neglected area mentioned above through the development of an efficient controller that can possibly incorporate all components of aerodynamic angles.

Most nonlinear plants, on the other hand, frequently suffer rapid changes in structures and characteristics as a result of equipment breakdowns and environmental fluctuations. *Markovian Jump Systems (MJSs)* may be used to represent these dynamic changes [21]. Noticeably, *MJSs* have a finite number of subsystems, such as the Markov process. This is recognized as a key feature of *MJSs* because this can characterize some sudden variations. *MJSs* has been investigated by a large number of researchers, and a lot of results are available related to this field have been made, such as sliding mode control [22], stability analysis [23], Peak–to–peak fuzzy filtering [24], omnidirectional automated systems [25] and so on. Due to its benefits as a type of stochastic hybrid nonlinear system, fuzzy Markov jump systems (FMJSs) have gained global interest and have been used as a type of T–S fuzzy model. As a case in point, to ensure stochastic stability, an input-output method for discrete-time *FMJSs* was used in [26]. In [27], authors used a T–S fuzzy model to explain nonlinear Markov jump singularly perturbed systems, taking into consideration together H_∞ and passive performance. The effective dissipativity assessment of *FMJSs* with actuator failures was focused in [28]. The *HV* system is a complex nonlinear system so it is reasonable to design an *FMJS* model and control strategy to estimate stability and desired performance. This research is motivated by this key concern.

In modern years, the accuracy of mechanical systems has been improved by developing robust control strategies. In [29], *ARC* has been applied and functioned in a wide range of motor fields to deal with external disturbances and parametric uncertainties simultaneously. Based on the theory in [29], the boundness of the controller is only valid when time-varying disturbances occur. Different nonlinear systems can benefit from the practical application of T–S fuzzy, for example, the process of oil catalytic cracking [30], rotary inverted pendulums [31], wireless networked control systems [32], Throttle body for electronic vehicles [33], and quadrotor unmanned aerial vehicles buck-boost converters [34]. According to [35], the sliding mode control can avoid singularities and so achieve zero convergence within a finite time. Accordingly, various effective control schemes have been detected for nonlinear systems based on these excellent works, such as *model predictive control (MPC)* [36], *LPV gains scheduling control* (LPV-G) [37], *robust tracking control* (RTC) [38], and so on. More papers have included studies into the nonlinear control for the subject of mechanical engineering in recent years, making it the focal point of this field of study.

In this article, to design fuzzy control systems better, a class of *Sustainable Hypersonic Vehicles (SHVs)* with an H_∞ performance index is examined. Here are some highlights of contributions and novelties. *Firstly*, we established a novel model based on *T–S fuzzy control*, and then we applied the stochastic process to nonlinear systems with H_∞ control of the *SHVs*. *Secondly*, we integrated this estimation error among the fuzzy model and nonlinear system, as well as this two–level structured fuzzy model for *SHVs*, with the fuzzy control design. In fact, this influence of the approximation error on nonlinear control systems can degrade their stability and control performance. Furthermore, we used a combined Lyapunov function and stochastic stability to provide a systematic approach. The aim of doing so was to construct a resilient fuzzy control that keeps the closed–loop system's H_∞ gain in a specified value in the presence of limited disturbances. Finally, a robustness analysis of the disturbance level and force moments was made to ensure that our suggested method is successful.

The remaining part of the article is defined as follows: In Section *2*, some mathematical formulation for *SHVs* is thoroughly discussed. *SHVs* system descriptions are defined and discussions on the concept of a model, as well as some stability aspects, are also provided in Section *3*. Simulations made in this research are included in Section *4* to demonstrate their effectiveness. Finally, the conclusions drawn and recommendations for future studies are provided as well.

We as the authors provide the definition before moving on to the main mathematical modeling. This helps determine the main conclusions of the study.

Definition 1 *The Markov Process Fuzzy System (*MPFS*) (38) with* $w \equiv 0$ *is called to be stochastically stable if all*

initial conditions (p_0, r_0) *are admissible, and there exists a fuzzy control law (34) satisfying*

$$\mathcal{E}\left[\int_0^\infty p(t,p_0,r_0,u)^T p(t,p_0,r_0,u)dt|p_0,r_0\right] \leq p_0^T \mathcal{M} p_0 \tag{1}$$

for some matrices $\mathcal{M} = \mathcal{M}^T$, $\mathcal{M} > 0$ *of proper dimensions.*

2 Preliminary results of a problem formulation

2.1 Formulation of the problem

The sustainable hypersonic vehicle's initial nonlinear reentry motion equations can be stated as follows [46]:

$$\begin{aligned}
\dot{\theta}_\alpha &= \psi_q - \tan\theta_\beta(\psi_p\cos\theta_\alpha + \psi_r\sin\theta_\alpha) - \theta_{11}(\dot{\gamma} - \dot{\varphi}\cos\mathcal{X} - \theta_{12}(\cos\varphi\sin\mathcal{X})) \\
&+ \theta_{11}(\dot{\mathcal{X}}\cos\gamma - \dot{\varphi}\cos\mathcal{X}\sin\gamma + \theta_{12}\cdot(\cos\varphi\cos\mathcal{X}\sin\gamma - \sin\varphi\cos\gamma)) \\
\dot{\theta}_\beta &= \psi_p\sin\theta_\alpha - \psi_r\cos\theta_\alpha + \sin\theta_\mu(\dot{\gamma} - \dot{\varphi}\cos\mathcal{X} - \theta_{12}\cos\varphi\sin\mathcal{X})) \\
&+ \cos\theta_\mu\cdot(\dot{\mathcal{X}}\cos\gamma - \dot{\varphi}\cos\mathcal{X}\sin\gamma + \theta_{12}\cdot(\cos\varphi\cos\mathcal{X}\sin\gamma - \sin\varphi\cos\gamma)) \\
\dot{\theta}_\mu &= -\psi_q\sin\theta_\beta - \cos\theta_\beta(\psi_p\cos\theta_\alpha + \psi_r\sin\theta_\alpha) + \dot{\theta}_\alpha\sin\theta_\beta - \dot{\mathcal{X}}\cdot\sin\gamma - \varphi\sin\mathcal{X}\cos\gamma \\
&+ \theta_{12}(\cos\varphi\cos\mathcal{X}\cos\gamma + \sin\varphi\cos\gamma)
\end{aligned} \tag{2}$$

where

$$\theta_{11} = \frac{\cos\theta_\mu}{\cos\theta_\beta}, \qquad \theta_{12} = (\dot{\lambda} + \omega_e) \tag{3}$$

In the above eq., θ_α presents the angle of attack, θ_β denotes the sideslip angle, and θ_μ presents the bank angle. Now, we present the rate of rotation of all three aspects from [46],which is given below:

$$\begin{bmatrix} \dot{\psi}_p \\ \dot{\psi}_q \\ \dot{\psi}_r \end{bmatrix} = \begin{bmatrix} \mathcal{I}^{\psi_p}_{\psi_p\psi_q} & \mathcal{I}^{\psi_p}_{\psi_q\psi_r} & 0 & 0 & 0 & 0 & 0 & g^{\psi_p}_n & g^{\psi_p}_\ell \\ 0 & 0 & 0 & \mathcal{I}^{\psi_q}_{\psi_p\psi_r} & \mathcal{I}^{\psi_q}_{\psi_r\psi_r} & \mathcal{I}^{\psi_q}_{\psi_p\psi_p} & g^{\psi_q}_m & 0 & 0 \\ \mathcal{I}^{\psi_r}_{\psi_p\psi_q} & \mathcal{I}^{\psi_r}_{\psi_q\psi_r} & 0 & 0 & 0 & 0 & 0 & g^{\psi_r}_n & g^{\psi_r}_\ell \end{bmatrix} \begin{bmatrix} \psi_p\psi_q \\ \psi_q\psi_r \\ \psi_p\psi_r \\ \psi_r^2 \\ \psi_p^2 \\ m \\ n \\ \ell \end{bmatrix} \tag{4}$$

ψ_p denotes the bank angle rate of rotation, ψ_q indicates the angle of attack rate, and ψ_r is the sideslip angle rate of rotation. In particle kinematics, the variables $(V, \gamma, \mathcal{X})$ and (R, φ, λ) are connected to vehicle position and velocity. $\mathcal{I}^\square_\square$ and $g^\square_\square$ are persistent coefficients that influence the vehicle's moment of inertia, and ω_e represents the earth's rotation angular rate. Despite this, unlike the longitude plane dynamics of air-breathing hypersonic vehicles and the *HV* re-entry dynamics, this kind of *HV* re-entry dynamics does not individually include this dynamics of 6 attitude variables in 3 channels. However, it also has a strong coupling and complicated nonlinearity because it couples these trajectory variables $[\gamma, \mathcal{X}]$ with the earth rotation angular rate ω_e.

Because one of the main goals in this research is to develop a fuzzy model for *SHV* reentry attitude dynamics, the differential equations given in (2) have a generic method that must be recast into a control-oriented form. The transforming step in motion equations (2) for this control–oriented model can be frequently neglected or a separate model will be explicitly supplied in prior studies. The focus of the current research is to investigate this process in detail.

In comparison to the motions with variables $\begin{bmatrix} \theta_\alpha \\ \theta_\beta \\ \theta_\mu \\ \psi_p \\ \psi_q \\ \psi_r \end{bmatrix}$ in reentry dynamics equation (2), when sections of ω_e are

considered, only a minor effect on system dynamics is seen; instead, clear effects shall act on these motions for trajectory variables in re-entry trajectory equations to trajectory optimization and guidance research. As a result, in the following explanation, the parts of the earth's rotation angular rate ω_e shall be removed. Thus, in effect, the trajectory equations can be created through $[\dot{\lambda}, \dot{\varphi}, \dot{\gamma}, \dot{\mathcal{X}}]$, and the following truth will be established when the value of ω_e is considered null in (2).

$$\begin{aligned} \mathcal{F}_\gamma &= VM(\dot{\gamma} - \dot{\varphi}\cos\mathcal{X} - \theta_{12}\cos\varphi\sin\mathcal{X}) \\ \mathcal{F}_\mathcal{X} &= VM\left(\cos\varphi\cos\mathcal{X}\sin\gamma - \sin\varphi\cos\gamma\right) \\ \mathcal{F}_\mathcal{X}\tan\gamma &= VM\left(-\dot{\mathcal{X}}\cdot\sin\gamma - \dot{\varphi}\sin\mathcal{X}\cos\gamma + \theta_{12}\cdot(\cos\varphi\cos\mathcal{X}\cos\gamma + \sin\varphi\cos\gamma)\right) \end{aligned} \tag{5}$$

Where $\mathcal{F}_\gamma$ and $\mathcal{F}_\mathcal{X}$ present the aerodynamic force spoiler for the velocity coordinate system, which are described as:

$$\begin{bmatrix} \mathcal{F}_\gamma \\ \mathcal{F}_\mathcal{X} \end{bmatrix} = \begin{bmatrix} -\mathcal{Y} & \mathcal{L} & \mathcal{M}g \\ -\mathcal{L} & -\mathcal{Y} & 0 \end{bmatrix} \begin{bmatrix} \sin\theta_\mu \\ \cos\theta_\mu \\ \cos\gamma \end{bmatrix} \tag{6}$$

By replacing eq. (6), re-entry dynamics eq. (2) shall be denoted as

$$\begin{aligned} \dot{\theta}_\alpha &= \psi_q - \tan\theta_\beta(\psi_p\cos\theta_\alpha + \psi_r\sin\theta_\alpha) - \tfrac{\cos\theta_\mu}{\cos\theta_\beta}\tfrac{\mathcal{F}_\gamma}{VM} + \tfrac{\cos\theta_\mu}{\cos\theta_\beta}\tfrac{\mathcal{F}_\mathcal{X}}{VM} \\ \dot{\theta}_\beta &= \psi_p\sin\theta_\alpha - \psi_r\cos\theta_\alpha + \sin\theta_\mu\tfrac{\mathcal{F}_\gamma}{VM} + \cos\theta_\mu\tfrac{\mathcal{F}_\mathcal{X}}{VM} \\ \dot{\theta}_\mu &= -\psi_q\sin\theta_\beta - \cos\theta_\beta(\psi_p\cos\theta_\beta + \psi_r\sin\theta_\alpha) + \dot{\theta}_\alpha\sin\theta_\beta - \tfrac{\mathcal{F}_\mathcal{X}}{VM}\tan\gamma \end{aligned} \tag{7}$$

In the same consequences:

$$\begin{bmatrix} \dot{\psi}_p \\ \dot{\psi}_q \\ \dot{\psi}_r \end{bmatrix} = \begin{bmatrix} \mathcal{I}^{\psi_p}_{\psi_p\psi_q} & \mathcal{I}^{\psi_p}_{\psi_q\psi_r} & 0 & 0 & 0 & 0 & 0 & g^{\psi_p}_n & g^{\psi_p}_\ell \\ 0 & 0 & 0 & \mathcal{I}^{\psi_q}_{\psi_p\psi_r} & \mathcal{I}^{\psi_q}_{\psi_r\psi_r} & \mathcal{I}^{\psi_q}_{\psi_p\psi_p} & g^{\psi_q}_m & 0 & 0 \\ \mathcal{I}^{\psi_r}_{\psi_p\psi_q} & \mathcal{I}^{\psi_r}_{\psi_q\psi_r} & 0 & 0 & 0 & 0 & 0 & g^{\psi_r}_n & g^{\psi_r}_\ell \end{bmatrix} \begin{bmatrix} \psi_p\psi_q \\ \psi_q\psi_r \\ \psi_p\psi_r \\ \psi_r^2 \\ \psi_p^2 \\ m \\ n \\ \ell \end{bmatrix} \tag{8}$$

Now, we present the force with their moment as follows:

$$\begin{aligned} \begin{bmatrix} \mathcal{Y} & \mathcal{L} & \ell & m & n \end{bmatrix} &= \begin{bmatrix} \mathcal{C}_\mathcal{Y} & \mathcal{C}_\mathcal{L} & \mathcal{C}_\ell b & \mathcal{C}_m c & \mathcal{C}_n b \end{bmatrix} \mathcal{QS} \\ \mathcal{C}_\mathcal{Y} &= \mathcal{C}_{\mathcal{Y},\theta_\beta}\theta_\beta + \mathcal{C}_{\mathcal{Y},\delta_e}\delta_e + \mathcal{C}_{\mathcal{Y},\delta_a}\delta_a + \mathcal{C}_{\mathcal{Y},\delta_{\psi_r}}\delta_{\psi_r} \\ &= f_\mathcal{Y}(\theta_\alpha, \theta_\beta, \delta_e, \delta_a, \delta_{\psi_r}) \\ \mathcal{C}_\mathcal{L} &= \mathcal{C}_{\mathcal{L},\theta_\alpha} + \mathcal{C}_{\mathcal{L},\delta_e}\delta_e + \mathcal{C}_{\mathcal{L},\delta_a}\delta_a \\ &= f_\mathcal{L}(\theta_\alpha, \theta_\beta, \delta_e, \delta_a, \delta_{\psi_r}) \\ \mathcal{C}_\ell &= \mathcal{C}_{\ell_{\theta_\beta}}\theta_\beta + \mathcal{C}_{\ell,\delta_e}\delta_e + \mathcal{C}_{\ell,\delta_a}\delta_a + \mathcal{C}_{\ell,\delta_r}\delta_r \\ &= f_\ell(\theta_\alpha, \theta_{\theta_\alpha}, \delta_e, \delta_a, \delta_{\psi_r}) \\ \mathcal{C}_m &= \mathcal{C}_{m_{\theta_\alpha}} + \mathcal{C}_{m,\delta_e}\delta_e + \mathcal{C}_{m,\delta_a}\delta_a + \mathcal{C}_{m,\delta_{\psi_r}}\delta_{\psi_r} \\ &= f_m(\theta_\alpha, \theta_\beta, \delta_e, \delta_a, \delta_{\psi_r}) \\ \mathcal{C}_n &= \mathcal{C}_{n_{\theta_\beta}}\theta_\beta + \mathcal{C}_{n,\delta_e}\delta_e + \mathcal{C}_{n,\delta_a}\delta_a + \mathcal{C}_{n,\delta_{\psi_r}}\delta_{\psi_r} \\ &= f_n(\theta_\alpha, \theta_\beta, \delta_e, \delta_a, \delta_{\psi_r}) \end{aligned} \tag{9}$$

Substituting eq. (9) into eqs. (7) & (8) and denoting $\mho = \begin{bmatrix} \theta_\alpha \\ \theta_\beta \\ \theta_\mu \end{bmatrix}$ and $\omega = \begin{bmatrix} \psi_p \\ \psi_q \\ \psi_r \end{bmatrix}$, nonlinear re-entry plant eq. (6) can be inferred as the below nonlinear affine model:

$$\begin{bmatrix} \dot{\mho} \\ \dot{\omega} \end{bmatrix} = \begin{bmatrix} \mathrm{f}_s + \mathrm{g}_{s1}\omega + \mathrm{g}_{s2}\delta \\ \mathrm{f}_f + \mathrm{g}_f\mathrm{M}_c \end{bmatrix} = \begin{bmatrix} \mathrm{f}_s + \mathrm{g}_{s1}\omega + \mathrm{g}_{s2}\delta \\ \mathrm{f}_f + \mathrm{g}_f\cdot\mathrm{g}_{f\delta}\cdot\delta \end{bmatrix} \tag{10}$$

where

$$
\begin{aligned}
\mathrm{f}_s &= \tfrac{1}{VM}\begin{bmatrix} \frac{-\mathcal{C}_{\mathcal{L},\theta_\alpha}\mathcal{QS}+\mathrm{M}g\cos\gamma\cos\theta_\mu}{\cos\theta_\beta} \\ -\mathcal{C}_{\mathcal{Y},\theta_\beta}\theta_\beta\mathcal{QS} - Mg\cos\gamma\sin\theta_\mu \\ \mathcal{C}_{\mathcal{L},\theta_\alpha}\mathcal{QS}(\tan\theta_\beta+\cos\theta_\mu)+\mathcal{C}_{\mathcal{Y},\theta_\beta}\theta_\beta\mathcal{QS}\cos\theta_\beta - Mg\cos\gamma\cos\theta_\mu\tan\theta_\beta \end{bmatrix} \\
\mathrm{g}_{s1} &= \begin{bmatrix} -\tan\theta_\beta\cos\theta_\alpha & 1 & -\tan\theta_\beta\sin\theta_\alpha \\ \sin\theta_\alpha & 0 & -\cos\theta_\alpha \\ -\sec\theta_\beta\cos\theta_\alpha & 0 & -\sec\theta_\beta\sin\theta_\alpha \end{bmatrix} \\
\mathrm{g}_{s2} &= \tfrac{\mathcal{QS}}{VM}\begin{bmatrix} \frac{\mathcal{C}_{\mathcal{L},\delta_e}}{\cos\theta_\beta} & \frac{\mathcal{C}_{\mathcal{L},\delta_a}}{\cos\theta_\beta} & \frac{\mathcal{C}_{\mathcal{L},\delta_{\psi_r}}}{\cos\theta_\beta} \\ \mathcal{C}_{\mathcal{Y},\delta_e} & \mathcal{C}_{\mathcal{Y},\delta_a} & \mathcal{C}_{\mathcal{Y},\delta_{\psi_r}} \\ \mathcal{C}_{\mathcal{L},\delta_e}(\tan\theta_\beta+\cos\theta_\mu)+\mathcal{C}_{\mathcal{Y},\delta_e}\cos\theta_\beta & \mathcal{C}_{\mathcal{L},\delta_a}(\tan\theta_\beta+\cos\theta_\mu)+\mathcal{C}_{\mathcal{Y},\delta_a}\cos\theta_\beta & \mathcal{C}_{\mathcal{L},\delta_{\psi_r}}(\tan\theta_\beta+\cos\theta_\mu)+\mathcal{C}_{\mathcal{Y},\delta_{\psi_r}}\cos\theta_\beta \end{bmatrix}
\end{aligned}
$$

$$
\begin{aligned}
\mathrm{f}_f &= \begin{bmatrix} \mathcal{I}^{\psi_p}_{\psi_p\psi_q}\psi_p\psi_q + \mathcal{I}^{\psi_p}_{\psi_q\psi_r}\psi_q\psi_r + g^{\psi_p}_{\ell}\ell_A \\ \mathcal{I}^{\psi_q}_{\psi_p\psi_p}\psi_p^2 + \mathcal{I}^{\psi_q}_{\psi_r\psi_r}\psi_r^2 + \mathcal{I}^{\psi_q}_{\psi_p\psi_r}\psi_p\psi_r + g^{\psi_q}_{m}m_A \\ \mathcal{I}^{\psi_r}_{\psi_q\psi_r}\psi_q\psi_r + \mathcal{I}^{\psi_r}_{\psi_p\psi_q}\psi_p\psi_q + g^{\psi_r}_{n}n_A \end{bmatrix}, \\
\mathrm{g}_f &= \begin{bmatrix} \mathrm{g}^{\psi_p}_{\ell} & 0 & \mathrm{g}^{\psi_p}_{n} \\ 0 & \mathrm{g}^{\psi_q}_{m} & 0 \\ \mathrm{g}^{\psi_r}_{\ell} & 0 & \mathrm{g}^{\psi_r}_{n} \end{bmatrix}, \quad \delta = \begin{bmatrix} \delta_e \\ \delta_a \\ \delta_r \end{bmatrix}, \\
\mathrm{g}_{f\delta} &= \mathcal{QS}\begin{bmatrix} bC_{\ell,\delta_e} & b\mathcal{C}_{\ell,\delta_a} & b\mathcal{C}_{\ell,\delta_{\psi_r}} \\ \mathrm{g}_{m,\delta_e} & \mathrm{g}_{m,\delta_a} & \mathrm{g}_{m,\delta_{\psi_r}} \\ b\mathcal{C}_{n,\delta_e}+X_{cg}\mathcal{C}_{\mathcal{Y},\delta_e} & b\mathcal{C}_{n,\delta_a}+X_{cg}\mathcal{C}_{\mathcal{Y},\delta_a} & b\mathcal{C}_{n,\delta_{\psi_r}}+X_{cg}\mathcal{C}_{\mathcal{Y},\delta_{\psi_r}} \end{bmatrix}
\end{aligned} \tag{11}
$$

$\mathrm{g}_{s2}\delta$ has no influence on the variables $\mho = \begin{bmatrix} \theta_\alpha \\ \theta_\beta \\ \theta_\mu \end{bmatrix}$ in part since the aerodynamic force created through the rudder is considerably smaller than the force moment produced by the vehicle body eq. (10). As a result, recasting equation eq. (10) produces:

$$
\begin{bmatrix} \dot{\mho} \\ \dot{\omega} \end{bmatrix} = \begin{bmatrix} \mathrm{g}_{s1}\omega \\ \mathrm{f}_{f1} \end{bmatrix} + \begin{bmatrix} 0 \\ \mathrm{g}_f \end{bmatrix}\mathrm{M}_c + \begin{bmatrix} \mathrm{f}_s \\ \mathrm{f}_{f2} \end{bmatrix} \tag{12}
$$

Let

$$
\begin{aligned}
p(t) &= \begin{bmatrix} \mho \\ \omega \end{bmatrix} = \begin{bmatrix} \theta_\alpha \\ \theta_\beta \\ \theta_\mu \\ \psi_p \\ \psi_q \\ \psi_r \end{bmatrix}, \qquad u(t) = \mathcal{M}_c \\
\mathrm{f}(p) &= \begin{bmatrix} \mathrm{g}_{s1}\omega \\ \mathrm{f}_{f1} \end{bmatrix} = \begin{bmatrix} 0_{3\times 3} \\ \mathrm{g}_f \end{bmatrix}, \qquad \nabla(p) = \begin{bmatrix} \mathrm{f}_s \\ \mathrm{f}_{f2} \end{bmatrix}
\end{aligned}
$$

Finally, we can rewrite the affine model with the nonlinearity:

$$
\dot{p}(t) = \mathrm{f}(p) + G_p u(t) + \nabla(p), \tag{13}
$$

in which

$$
\begin{aligned}
\mathrm{f}(p) &= \begin{bmatrix} \mathrm{f}_1 \\ \mathrm{f}_2 \\ \mathrm{f}_3 \\ \mathrm{f}_4 \\ \mathrm{f}_5 \\ \mathrm{f}_6 \end{bmatrix} = \begin{bmatrix} -\psi_p \tan\theta_\beta \cos\theta_\alpha + \psi_q - \psi_r \tan\theta_\beta \sin\theta_\alpha \\ \psi_p \sin\theta_\alpha - \psi_r \cos\theta_\alpha \\ -\psi_p \sec\theta_\beta \cos\theta_\alpha - \psi_r \sec\theta_\beta \sin\theta_\alpha \\ \mathcal{I}^{\psi_p}_{\psi_p\psi_q}\psi_p\psi_q + \mathcal{I}^{\psi_p}_{\psi_q\psi_r}\psi_q\psi_r \\ \mathcal{I}^{\psi_q}_{\psi_p\psi_p}\psi_p^2 + \mathcal{I}^{\psi_q}_{\psi_r\psi_r}\psi_r^2 + \mathcal{I}^{\psi_q}_{\psi_p\psi_r}\psi_p\psi_r \\ \mathcal{I}^{\psi_r}_{\psi_q\psi_r}\psi_q\psi_r + \mathcal{I}^{\psi_r}_{\psi_p\psi_q}\psi_p\psi_q \end{bmatrix} \\
G_p &= \begin{bmatrix} & 0_{3\times 3} & \\ g_\ell^{\psi_p} & 0 & g_n^{\psi_p} \\ 0 & g_m^{\psi_q} & 0 \\ g_\ell^{\psi_r} & 0 & g_n^{\psi_r} \end{bmatrix}, \qquad (14) \\
\Delta(p) &= \begin{bmatrix} \frac{-\mathcal{C}_{\mathcal{L}_{\theta_\alpha}}\mathcal{QS} + Mg\cos\gamma\cos\theta_\mu}{VM\cos\theta_\beta} \\ \frac{-\mathcal{C}_{\mathcal{Y},\theta_\beta}\theta_\beta\mathcal{QS} - Mg\cos\gamma sin\theta_\mu}{MV} \\ \frac{\mathcal{C}_{\mathcal{L},\theta_\alpha}\mathcal{QS}(\tan\theta_\beta + \cos\theta_\mu) + \mathcal{C}_{\mathcal{Y},\theta_\beta}\theta_\beta\mathcal{QS}\cos\theta_\beta - Mg\cos\gamma\cos\theta_\mu\tan\theta_\beta}{VM} \\ g_\ell^{\psi_p}\ell_A + g_n^{\psi_p}n_A \\ g_m^{\psi_q}m_A \\ g_\ell^{\psi_r}\ell_A + g_n^{\psi_r}n_A \end{bmatrix}
\end{aligned}
$$

$\nabla(p)$ is the unreliable parameter associated with the vehicle's aerodynamics. The control input $u(t)$ is defined through respect for the control surface deflections $\delta = \begin{bmatrix} \delta_e \\ \delta_a \\ \delta_r \end{bmatrix}$.

Remark 1 *In the dynamics of a sustainable hypersonic vehicle, authors considered reentry motion equations with nonlinear behavior. In terms of system modeling, the authors thought highly of three different angles (bank of angles, bank of rotation, and slide slip angle). So, we as the authors introduced the Markov jump process for the i^{th} subsystem with fuzzy systems to deal with randomness.*

2.2 Linearization Technique with Fuzzy

2.2.1 Problem Statement

As shown in eq. (13), the *SHVs* reentry dynamics include distinct traits of multi–variable coupling and high–order nonlinearity, that make direct decoupling and controlling challenging. The homogeneous fuzzy T–S models are intended to be built from the truth dynamic model to tackle this problem eq. (13). The unknown term $\nabla(p)$ is ignored in the next discussion because that could be handled through a controller design method for the H_∞ specification.

Eq. (13) is expressed as follows:

$$\dot{p}(t) = \mathrm{f}(p) + G_p u(t) = F(p,u) \qquad (15)$$

Where $G_p \in \mathbf{R}^{n\times m}$ and $F(p,u) = [F_1, F_2, \cdots, F_n]^T$. Increasing $F(p,u)$ through the median of Taylor's series for this neighborhood at an operating point of interest (p^j, u^j) produces

$$
\begin{aligned}
F(p,u) &\approx F(p^j,u^j) + [\tfrac{\partial F}{\partial p}]_{(p^j,u^j)}(p-p^j) + [\tfrac{\partial F}{\partial u}]_{(p^j,u^j)}(u-u^j) \\
&= \mathrm{f}(p^j) + G_p u^j + A_j(p-p^j) + G_p(u-u^j) \qquad (16) \\
&= \mathcal{A}_j p + \mathcal{B}_j u + (\mathrm{f}(p^j) - \mathcal{A}_j p^j)
\end{aligned}
$$

where

$$\mathcal{A}_j = [\tfrac{\partial F}{\partial p}]_{(p^j,u^j)} = \begin{bmatrix} \frac{\partial \mathrm{f}_1}{\partial p_1} & \frac{\partial \mathrm{f}_1}{\partial p_2} & \cdots & \frac{\partial \mathrm{f}_1}{\partial p_n} \\ \frac{\partial \mathrm{f}_2}{\partial p_1} & \frac{\partial \mathrm{f}_2}{\partial p_2} & \cdots & \frac{\partial \mathrm{f}_2}{\partial p_n} \\ \vdots & \vdots & & \vdots \\ \frac{\partial \mathrm{f}_n}{\partial p_1} & \frac{\partial \mathrm{f}_n}{\partial p_2} & \cdots & \frac{\partial \mathrm{f}_n}{\partial p_n} \end{bmatrix}_{(p^j)} \qquad (17)$$

is known as the *Jacobian matrix* of $\mathrm{f}(p)$, $\mathcal{B}_j = [\partial F/\partial u]_{(p^j,u^j)} = \mathrm{G}_p$, and $\mu_j = \mathrm{f}(p^j) - \mathcal{A}_j p^j$.
As mentioned, the bias factor μ_j is not always zero; using Taylor's expansion approach, homogeneous models $\dot{p} = F(p,u) = \mathcal{A}_j p + \mathcal{B}_j u$ can only be generated since the truth model when $\mu_j = 0$. Taylor's growth approach may also be recycled to linearize local nonlinear sectors in multi-variable decoupling in a conventional situation. A non–zero μ_j, on the other hand, poses the same difficulty. The nonlinear term $\mathcal{I}^{\psi_p}_{\psi_p\psi_q}\psi_p\psi_q$ in eq. (13) for example, can extend Taylor series around the nonzero operating point (ψ_{p_0}, ψ_{q_0}).

$$\begin{aligned} \psi_p\psi_q &= \psi_{p_0},\psi_{q_0} + \left[\tfrac{\partial(\psi_p\psi_q)}{\partial\psi_p}\right]_{(\psi_{p_0},\psi_{q_0})}(\psi_p - \psi_{p_0}) + [\tfrac{\partial(\psi_p\psi_q)}{\partial\psi_q}]_{(\psi_{p_0},\psi_{q_0})}(\psi_q - \psi_{q_0}) \\ &= \psi_{q_0}\psi_p + \psi_{p_0}\psi_q - \psi_{p_0}\psi_{q_0} \end{aligned} \tag{18}$$

Under normal conditions, $\psi_{p_0}\psi_{q_0} \neq 0$, which gives a linear model that cannot be designed for the neighborhood of (ψ_{p_0}, ψ_{q_0}).
This potential nonzero term μ_j in (16) turns this nonlinear system into a native affine subsystem by these operating points, increasing the challenge of designing a closed–loop controller to the nonlinear system at a certain level.

2.2.2 Matrix Linearization with the Jacobian Process

For this scenario, the additional linearization processes have been implemented in re-design from the creative one into homogeneous models for the vicinity of the non–zero operating points of interest. Which is, to find constant matrices $\mathcal{A}$ and $\mathcal{B}$ that, in the neighborhood of non–equilibrium operating points, $\mathfrak{x}^0$ produces

$$\mathrm{f}(p) + \mathrm{g}(p)u \approx \mathcal{A}p + \mathcal{B}u \tag{19}$$

And point $\mathfrak{x}^0$ fulfills

$$\mathrm{f}(p^0) + \mathrm{g}(p^0)u \approx \mathcal{A}p^0 + \mathcal{B}u \tag{20}$$

Since formula (19), it could be deducted that

$$\mathcal{B} = \mathrm{g}(p) \tag{21}$$

Subtracting formula (20) from formula (19) yields

$$[\mathrm{f}(p) - \mathrm{f}(p^0)] + [\mathrm{g}(p) - \mathrm{g}(p^0)]u = \mathcal{A}(p - p^0) \tag{22}$$

Form eq. (22), the arbitrary value of u is:

$$\mathrm{g}(p) = \mathrm{g}(p^0) \tag{23}$$

Finally,

$$\mathcal{B} = \mathrm{g}(p^0) \tag{24}$$

Presented $\mathcal{A}_j = [a_1 \quad a_2 \quad \cdots \quad a_n]^T$ is the i^{th} subsystem matrix linearized about the operating point $\mathfrak{x}^j$, here a_i^T is a row vector for the subsystem matrix $\mathcal{A}_j$. The vector in the subsystem matrix $\mathcal{A}_j$ produces

$$a_i = \nabla \mathrm{f}_i(p^j) + \tfrac{\mathrm{f}_i(p^j) - (p^j)^T\nabla\mathrm{f}_i(p^j)}{\|p^j\|^2}, \quad i = 1,2,\cdots,n, \quad i = 1,2,\cdots,r. \tag{25}$$

Where, $\mathrm{f}_i(p^j)$ is a value for the nonlinear function $\mathrm{f}_i(p)$ at the point p^j, and the column vector $\nabla\mathrm{f}_i(p^j)$ is the gradient of $\mathrm{f}_i(p)$ assessed at point p^j. Therefore, an integrated matrix form outcome shall be deduced as

$$\mathcal{A}_j = [a_1 \quad a_2 \quad \cdots \quad a_n]^T = J(\mathrm{f}(p^j)) + (p^j \cdot Z_j)^T. \tag{26}$$

Here, $Z_j = (1/\|p^j\|^2)([\mathrm{f}(p^j)]^2 - (p^j)^T[J(\mathrm{f}(p^j))]^T)$, $i = 1,2,\cdots,n$, $\quad i = 1,2,\cdots,r$, and the *Jacobian matrix* of $\mathrm{f(p)} = [\mathrm{f}_1, \mathrm{f}_2, \cdots, \mathrm{f}_n]^T$ is

$$J(\mathrm{f}) = \begin{bmatrix} \frac{\partial \mathrm{f}_1}{\partial p_1} & \frac{\partial \mathrm{f}_1}{\partial p_2} & \cdots & \frac{\partial \mathrm{f}_1}{\partial p_n} \\ \frac{\partial \mathrm{f}_2}{\partial p_1} & \frac{\partial \mathrm{f}_2}{\partial p_2} & \cdots & \frac{\partial \mathrm{f}_2}{\partial p_n} \\ \vdots & \vdots & & \vdots \\ \frac{\partial \mathrm{f}_n}{\partial p_1} & \frac{\partial \mathrm{f}_n}{\partial p_2} & \cdots & \frac{\partial \mathrm{f}_n}{\partial p_n} \end{bmatrix} \tag{27}$$

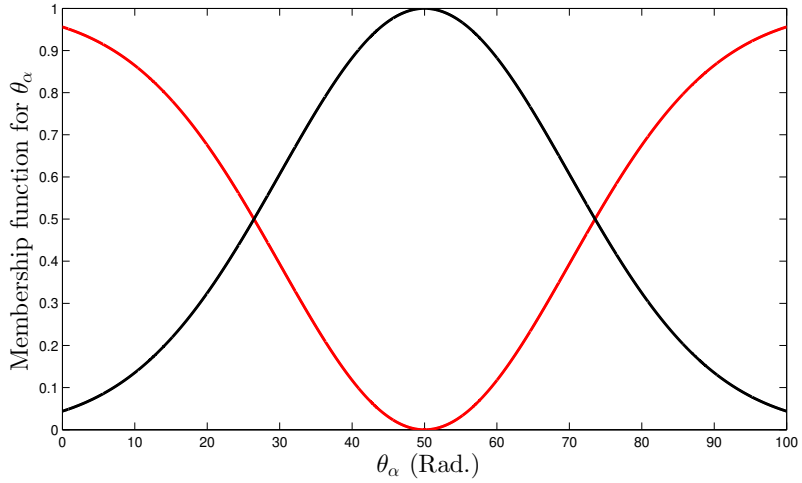

(a) Angle of attack θ_α

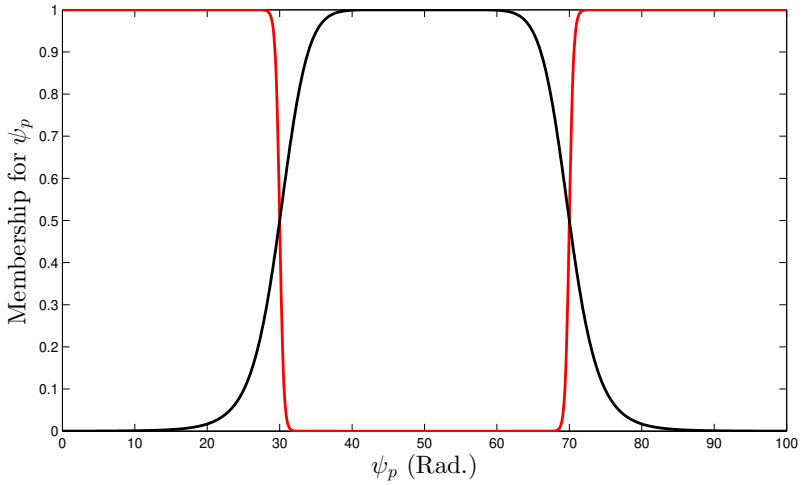

(b) Angular rate of rotation ψ_p

Figure 1: The Membership functions for (a) Attack Angle of θ_α, (b) Angular rate of rotation ψ_p, respectively [46].

In summary, for each operational point of interest, local identical models that approximate the unique plant are generated. The subsystem control matrices obtained with Taylor's expansion technique on equilibrium topics remain the same as those obtained with this Jacobian matrix linearization technique on other operating topics. This is not difficult to understand.

Remark 2 *According to the aforementioned study, the focus of this part is placed on homogeneous T–S fuzzy modeling for reentry dynamics plants (13). The need of creating an accurate fuzzy model for a high–dimensional control system would lead to the inclusion of extra premise variables, thereby resulting in issues such as the curse of dimension and rule explosion. The complicated formulation is impractical for application to hypersonic vehicles, even though the accurate fuzzy model shows good approximation with the actual plant. Apart from the potential application issue, adding additional fuzzy subsystems, particularly for high–order dynamic systems would unavoidably raise the complexity and conservativeness of controller design, leading to more system synthesis issues. As a result, those aforementioned issues were excluded from the local fuzzy modeling for SHVs discussed in this part by using proper fuzzy rules and premise variable selection to better achieve maximum modeling accuracy.*

3 Problem Formulation for Sustainable Hypersonic Vehicle

3.1 T-S Modelling with Stochastic Control for Nonlinear Model

Let's consider the *Markovian process nonlinear systems (MPNLs)* with the probability space with the help of differential equations:

$$\dot{p} = \mathrm{f}(p, r) + g(p, r)u + w; \quad p(0) = p_0; \quad r(0) = r_0 \tag{28}$$

where $p \in \mathbf{R}^n$ is a state vector of the system, $u \in \mathbf{R}^m$ is a control input vector, and $\omega \in \mathbf{R}^n$ is a bounded external disturbance fitting to $\mathbf{L}_2[0, \infty)$. For the continuous–time Markovian method, we denoted the symbol r over the finite space state presented by $\mathbf{S} = \{1, 2, \cdots, N\}$. Furthermore, p_0 and r_0 are primary conditions for this state, leading to the jumping mode at time $t = 0$, separately.

In this stochastic process $\{r, t \geq 0\}$ where authors should determine this mode in the system for each time t is supposed to be defined from the possibility:

$$Pr\{r(t + \hbar) = j | r(t) = i\} = \begin{cases} \pi_{ij}\hbar + o(\hbar), & i \neq j \\ 1 - \pi_i\hbar + o(\hbar), & i = j \end{cases} \tag{29}$$

where

$$\underbrace{lim}_{\hbar \to 0}(o(\hbar)\hbar^{-1}) = 0, \quad \hbar > 0$$

$\pi_{ij} \geq 0$ is a probability rate among modes i and j, for $i \neq j; j \in \mathbb{S}$ and $\pi_i = -\pi_{ii} = \sum_{j=1, j\neq i}^{N} \pi_{ij}$.

The matrix $\prod = [\pi_{ij}], \quad i, j = 1, 2, \cdots \mathbf{N}$ is known as the *transition rate matrix*. We assume that the Markov process r had an initial distribution $\mu = (\mu_1, \mu_2, \cdots, \mu_N)$ with $\mu_i = Pr\{r_0 = i\}$.

Let $z \in \mathbf{R}$ presents the mode variable, while M_i denotes the crisp set, and N_{ijk} is a fuzzy set. The *MPFSs* were then used to represent the *MPNLs* (28) and (29). The top and lower levels of this fuzzy system were specified by crisp sets. N_{ijk} linked with the nonlinearities for the state vector x and M_i is associated with the jumps for the Markov method triggered by z. As a result, the i^{th} mode assumed by systems (28) and (29) is

Mode i**:** If z is $\mathbf{M}_i$, Then

Rule j**:** if p_1 is $\mathbf{N}_{ij1}$ and ... and p_n is $\mathbf{N}_{ijn}$
Then

$$\dot{p} = \mathcal{A}_{ij}p + \mathcal{B}_{ij}u + \omega, \quad i \in \mathbf{S}, \quad j = 1, 2, \cdots, R \tag{30}$$

where $\mathcal{A}_{ij}$ and $\mathcal{B}_{ij}$ are the known matrices with proper dimensions, R presents the number of inference rules to each mode, and variables $p_1, \cdots, p_n$ have consisted of the state vectors p. This part "$\mathcal{A}_{ij}p + \mathcal{B}_{ij}u + \omega$" is stated as a subsystem for each mode i related to rule j, and variables p and z on the principle part were known as premise variables. In these fuzzy systems, the IF–part for the *MPFS* can be referred to as the premise part, while this THEN–part, in contrast, yields the consequent portion. The same consequence, these premise variables shall be functions for the *state variables*, *exterior disturbances*, and/or *time*.
The complete *MPFS* is concluded by a fuzzy blending of subsystems, that were nominated according to the mode assumed by the Markov process, which is

$$\dot{p} = \sum_{i=1}^{N} m_i(z) \left[\sum_{j=1}^{R} n_{ij}(p)(\mathcal{A}_{ij}p + \mathcal{B}_{ij}u) \right] + \omega \tag{31}$$

where $m_i(z)$ presents the mode analyzer which follows $m_i(z) = 1$ when $r = i$, then $m_i(z) = 0$ for $j \neq i$, and $n_{ij}(p)$ are normalized membership functions given by

$$n_{ij}(p) = \frac{\prod_{k=1}^{n} N_{ijk}(p_k)}{\sum_{i=1}^{R} \prod_{k=1}^{n} N_{ijk}(p_k)} \tag{32}$$

Furthermore $N_{ijk}(p_k) \in [0,1]$ is the grade of membership of $p_k, k = 1, 2, \cdots, n$ in the fuzzy set N_{ijk}. The membership functions of the chosen premise variables are illustrated in Figure 1. In addition, seeing the fact that in (32) $N_{ijk}(p_k) \geq 0, j = 1, 2, \cdots, R$, we have $n_{ij}(x) \geq 0$ and $\sum_{j=1}^{R} n_{ij}(x) = 1$. The universe of discourse $\mathbb{X} : \mathbb{R}^n \times \mathbb{S} \to \mathbb{R}^n$ for the *MPFS* is given by

$$\mathbb{X} = \bigcup_{i=1}^{N} \mathbf{Mode}_i = \mathbf{Mode}_1 \cup \mathbf{Mode}_2 \cup \cdots \cup \mathbf{Mode}_N \mathbf{Mode}_i \cap \mathbf{mode}_l = \phi,\ i \neq l,\ l \in \mathbb{S}$$

Mode i**:** If z is M_i, Then

Rule j**:** if p_1 is N_{ij1} and ... and p_n is N_{ijn}
Then

$$u = -\mathcal{K}_{ij} p \quad i \in \mathbb{S}, \quad j = 1, 2, \cdots, R \tag{33}$$

where $\mathcal{K}_{ij} \in \mathbf{R}^{m \times n}$ are the feedback gain matrices. Therefore, the complete fuzzy controller becomes:

$$u = -\sum_{i=1}^{N} \sum_{j=1}^{R} m_i(z) n_{ij}(p) \mathcal{K}_{ij} p. \tag{34}$$

Considering that $m_i(z) m_k(z) = 0, i \neq k, i, k \in \mathbf{S}$, then substituting (33) in (31), results

$$\dot{p} = \sum_{i=1}^{N} m_i(z) \left[\sum_{j=1}^{R} \sum_{k=1}^{R} n_{ij}(p) n_{ik}(p) (\mathcal{A}_{ij} - \mathcal{B}_{ij} \mathcal{K}_{ik}) \right] p + \omega \tag{35}$$

Further computing

$$\sum_{j=1}^{R} \sum_{k=1}^{R} n_{ij}(p) n_{ik}(p) = \sum_{j=1}^{R} n_{ij}^2(p) + 2 \sum_{j<k}^{R} n_{ij}(p) n_{ik}(p) \tag{36}$$

and

$$\sum_{j=1}^{R} n_{ij}(p) = 1$$

system (35) shall be revised as

$$\dot{p} = \sum_{i=1}^{N} m_i(z) \left[\sum_{j=1}^{R} n_{ij}^2(p) \mathcal{G}_{ij} + 2 \sum_{j<k}^{R} n_{ij}(p) n_{ik}(p) \mathcal{H}_{ijk} \right] p + \omega \tag{37}$$

where

$$\begin{aligned} \mathcal{G}_{ij} &:= \mathcal{A}_{ij} - \mathcal{B}_{ij} \mathcal{K}_{ij} \\ \mathcal{H}_{ijk} &:= (1/2)(\mathcal{A}_{ij} - \mathcal{B}_{ij} \mathcal{K}_{ik} + \mathcal{A}_{ik} - \mathcal{B}_{ik} \mathcal{K}_{ij}) \end{aligned}$$

Therefore, systems (28) and (29) can be defined as an uncertain fuzzy system (38), where Λ_f and Λ_g were the approximating errors explained in (39) and (40), respectively, as displayed below.

$$\dot{p} = \sum_{i=1}^{N} m_i(z) \left[\sum_{j=1}^{R} n_{ij}^2(p) \mathcal{G}_{ij} + 2 \sum_{j<k}^{R} n_{ij}(p) n_{ik}(p) \mathcal{H}_{ijk} \right] p + \Lambda_f + \Lambda_g + \omega \tag{38}$$

$$\Lambda_f := \sum_{i=1}^{N} m_i(z) \left[\sum_{j=1}^{R} n_{ij}(p) (f(p,r) - \mathcal{A}_{ij} p) \right] \tag{39}$$

$$\Lambda_g := -\sum_{i=1}^{N} m_i(z) \left[\sum_{j=1}^{R} \sum_{k=1}^{R} n_{ij}(p) n_{ik}(p) (g(p,r) - \mathcal{B}_{ij}) \mathcal{K}_{ik} p \right] \tag{40}$$

Using the Definition 1 of $m_i(z) = 1$, when $z \in M_i$, that is, $r = i$, we assume there exist bounding matrices $\Delta\mathcal{A}_{ij}$ and $\Delta\mathcal{B}_{ij}$, $j = 1, 2, \cdots, R$ for each mode i such that

$$\begin{cases} \|\Lambda_f\| \leq \left\| \sum_{j=1}^{R} n_{ij}(p) \Delta\mathcal{A}_{ij} p \right\| \\ \|\Lambda_g\| \leq \left\| \sum_{j=1}^{R} \sum_{k=1}^{R} n_{ij}(p) n_{ik} p \Delta\mathcal{B}_{ij} \mathcal{K}_{ik} p \right\| \end{cases} \tag{41}$$

for more detail of all trajectories p.

$$\begin{cases} \Delta\mathcal{A}_{ij} &= \delta_{ij}\mathcal{A}_{qi} \\ \Delta\mathcal{B}_{ij} &= \eta_{ij}\mathcal{B}_{qi} \end{cases} \tag{42}$$

where

$$\|\eta_{ij}\| \leq 1, \qquad \|\delta_{ij}\| \leq 1, \qquad j = 1, 2, \cdots, R.$$

and $\mathcal{A}_{qi}$ and $\mathcal{B}_{qi}$ are matrices with proper dimensions and structure, that could be selected agreeing well with the system's nonlinearity.

Let us start the answer for the *MPFS* (38) that fuzzy control law (34) with the initial conditions p_0 & r_0.
Definition 1 is comparable to Markovian jump linear systems that have undetermined nonlinearities' stochastic stability. According to Definition 1, stochastic stability for the Markovian jump fuzzy system indicates that a feedback fuzzy control rule exists which asymptotically initiatives the state from any specific initial condition for the origin of mean square sense, implying this closed–loop system's asymptotic stability.

The construction of opinion gain vectors $\mathcal{K}_{ij}, i \in \mathbf{S}, j = 1, 2, \cdots, R$ to the fuzzy control rule (34) which stochastically stabilizes *MPFS* (5) and attenuates the influence of external disturbance ω is the topic addressed by us in this work. The H_∞ system norm was used to express the reduction of the external disturbance outcome. Let $\mathcal{T}_\zeta^\omega$ presents the transfer matrix of the system from ω to the controlled output $\zeta := \mathcal{S}(r)^{1/2}p$. Then, the H_∞ norm of $\mathcal{T}_\zeta^\omega$ will be:

$$\|T_\zeta^\omega\|_\infty = \frac{\mathcal{E}\|\zeta\|_{\mathcal{L}_2}}{\|\omega\|_{\mathcal{L}_2}}|_{\omega\in\mathcal{L}_2[0,T]} \tag{43}$$

Hence, eq. (43) yields $\|\mathcal{T}_\zeta^\omega\|_\infty < \gamma$ with the performance index γ to the suboptimal H_∞ control problem.

3.2 Robust Fuzzy Control Design

Using a coupled Lyapunov function, we proved that the *MPFS* can be robustly stabilized by stochastic means (38) in this section. We defined a stabilizing control issue in the context of *LMIs* in order to get a systematic fuzzy control design.

Theorem 1 *For the given system* MPFS *(38) with $\omega \equiv 0$ is stochastically stabilized with the fuzzy control law (34) for all admissible uncertainties, if there exists a matrix $\mathcal{P}_i = \mathcal{P}_i^T$, $\mathcal{P}_i > 0$ of proper dimensions satisfying:*

$$\begin{aligned} &2\mathcal{P}_i\mathcal{P}_i + \sum_{v=1}^{R}(\mathcal{B}_{qi}\mathcal{K}_{iv})^T(\mathcal{B}_{qi}\mathcal{K}_{iv}) + \sum_{l=1;l\neq i}^{N}\pi_{il}\mathcal{P}_l + \mathcal{A}_{qi}^T\mathcal{A}_{qi} < 0 \\ &\Big(\mathcal{G}_{ij} - \tfrac{1}{2}\pi_i\boldsymbol{I}\Big)^T\mathcal{P}_i + \mathcal{P}_i\Big(\mathcal{G}_{ij} - \tfrac{1}{2}\pi_i\boldsymbol{I}\Big); \qquad j = 1, \cdots, R \end{aligned} \tag{44}$$

$$\begin{aligned} &2\mathcal{P}_i\mathcal{P}_i + \sum_{v=1}^{R}(\mathcal{B}_{qi}\mathcal{K}_{iv})^T(\mathcal{B}_{qi}\mathcal{K}_{iv}) + \sum_{l=1;l\neq i}^{N}\pi_{il}\mathcal{P}_l + \mathcal{A}_{qi}^T\mathcal{A}_{qi} \\ &\Big(\mathcal{H}_{ijk} - \tfrac{1}{2}\pi_i\boldsymbol{I}\Big)^T\mathcal{P}_i + \mathcal{P}_i\Big(\mathcal{H}_{ijk} - \tfrac{1}{2}\pi_i\boldsymbol{I}\Big); \quad j < k; \quad j,k = 1, \cdots, R \end{aligned} \tag{45}$$

for all $i \in \mathbf{S}$

Proof: First, we should present the mode at time t be i, that is $r = i, i \in \mathbf{S}$. For the simplicity of notation, p presents the solution $p(t, p_0, r_0, u)$ of the *MPFS* (38) when $\omega \equiv 0$ with the initial condition (p_0, r_0) with fuzzy control law (34). Let's consider the candidate for the Lyapunov function as:

$$\mathcal{V}(p, r = i) = p^T\mathcal{P}_i p, \qquad \text{for all } i \in \mathbf{S} \tag{46}$$

with $\mathcal{P}_i = \mathcal{P}_i^T$, $\mathcal{P}_i > 0$ a positive–definite matrix of proper dimension. Then, apply the weak infinitesimal operator of (46) as

$$\mathcal{A}\{\mathcal{V}(p, r = i)\} := \lim_{\delta\to 0}\tfrac{1}{\delta}\Big\{\,\mathcal{E}[\mathcal{V}(p(t+\delta), r(t+\delta))|p, r = i] - \mathcal{V}(p, r = i)\,\Big\} \tag{47}$$

Using the idea of *Mariton*, it can be obtained

$$\begin{aligned}\mathcal{A}\{\mathcal{V}(p,i)\} &= \dot{p}^T \tfrac{\partial}{\partial p}\mathcal{V}(p,i) + \textstyle\sum_{l=1}^{N} \pi_{il}\mathcal{V}(p,l) \\ &= \dot{p}^T\mathcal{P}_i p + p^T\mathcal{P}_i\dot{p} + p^T\left(\textstyle\sum_{l=1}^{N}\pi_{il}\mathcal{P}_i\right)p\end{aligned} \tag{48}$$

Substituting eq. (38) in eq. (48) and using the fact that $m_i(z) = 1$ when $r = i$, it results

$$\begin{aligned}\mathcal{A}\{\mathcal{V}(p,i)\} &= p^T\Big[\textstyle\sum_{j=1}^{R} n_{ij}^2(p)(\mathcal{G}_{ij}^T\mathcal{P}_i + \mathcal{P}_i\mathcal{G}_{ij}) \\ &\quad +2\textstyle\sum_{j<k}^{R} n_{ij}(p)n_{jk}(p)(\mathcal{H}_{ijk}^T\mathcal{P}_i + \mathcal{P}_i\mathcal{H}_{ijk}) + \textstyle\sum_{l=1}^{R}\pi_{il}\mathcal{P}_i\Big]p \\ &\quad +(\Lambda_f)^T\mathcal{P}_i p + p^T\mathcal{P}_i(\Lambda_f) + (\Lambda_g)^T\mathcal{P}_i p + p^T\mathcal{P}_i(\Lambda_g)\end{aligned} \tag{49}$$

Using

$$\pi_i = -\pi_{ii} = \sum_{j=1, j\neq i}^{N} \pi_{ij}$$

Then, we can write eq. (49) as follows:

$$\begin{aligned}\mathcal{A}\{\mathcal{V}(p,i)\} &= p^T\Big\{\textstyle\sum_{j=1}^{R} n_{ij}^2(p)\left[\left(\mathcal{G}_{ij} - \tfrac{1}{2}\pi_i\mathbf{I}\right)\mathcal{P}_i + \mathcal{P}_i\left(\mathcal{G}_{ij} - \tfrac{1}{2}\pi_i\mathbf{I}\right)\right] + 2\textstyle\sum_{j<k}^{R} n_{ij}(p)n_{jk}(p) \\ &\quad \left[\left(\mathcal{H}_{ijk} - \tfrac{1}{2}\pi_i\mathbf{I}\right)^T\mathcal{P}_i + \mathcal{P}_i\left(\mathcal{H}_{ijk} - \tfrac{1}{2}\pi_i\mathbf{I}\right)\right] + \textstyle\sum_{l=1;l\neq i}^{R}\pi_{il}\mathcal{P}_i\Big\}p + (\Lambda_f)^T\mathcal{P}_i p \\ &+ p^T\mathcal{P}_i(\Lambda_f) + (\Lambda_g)^T\mathcal{P}_i p + p^T\mathcal{P}_i(\Lambda_g)\end{aligned} \tag{50}$$

Using the fact that

$$\begin{aligned}(\Lambda_f)^T\mathcal{P}_i p + p^T\mathcal{P}_i(\Lambda_f) &\leq (\Lambda_f)^T(\Lambda_f) + p^T\mathcal{P}_i\mathcal{P}_i p \\ (\Lambda_g)^T\mathcal{P}_i p + p^T\mathcal{P}_i(\Lambda_g) &\leq (\Lambda_g)^T(\Lambda_g) + p^T\mathcal{P}_i\mathcal{P}_i p\end{aligned}$$

Applying the weak infinitesimal operator given by eq. (50) satisfies:

$$\begin{aligned}\mathcal{A}\{\mathcal{V}(p,i)\} &\leq p^T\Big\{\textstyle\sum_{j=1}^{R} n_{ij}^2(p)\left[\left(\mathcal{G}_{ij} - \tfrac{1}{2}\pi_i\mathbf{I}\right)^T\mathcal{P}_i + \mathcal{P}_i\left(\mathcal{G}_{ij} - \tfrac{1}{2}\pi_i\mathbf{I}\right)\right] + 2\textstyle\sum_{j<k}^{R} n_{ij}(p)n_{jk}(p) \\ &\quad \left[\left(\mathcal{H}_{ijk} - \tfrac{1}{2}\pi_i\mathbf{I}\right)^T\mathcal{P}_i + \mathcal{P}_i\left(\mathcal{H}_{ijk} - \tfrac{1}{2}\pi_i\mathbf{I}\right)\right] + \textstyle\sum_{l=1;l\neq i}^{R}\pi_{il}\mathcal{P}_i\Big\}p \\ &+ (\Lambda_f)^T(\Lambda_f) + (\Lambda_g)^T(\Lambda_g) + 2p^T\mathcal{P}_i\mathcal{P}_i p\end{aligned} \tag{51}$$

Now, considering eq. (41) for $\Delta\mathcal{A}_{ij}$ and $\Delta\mathcal{B}_{ij}$ as in eq. (42), respectively, we get:

$$(\Lambda_f)^T(\Lambda_f) \leq p^T(\mathcal{A}_{qi}^T\mathcal{A}_{qi})p \tag{52}$$

and

$$(\Lambda_g)^T(\Lambda_g) \leq p^T\left(\textstyle\sum_{k=1}^{R} n_{ik}(p)\mathcal{B}_{qi}\mathcal{K}_{ik}\right) \times \left(\textstyle\sum_{k=1}^{R} n_{ik}(p)\mathcal{B}_{qi}\mathcal{K}_{ik}\right)p \tag{53}$$

Using the fact that:

$$\sum_{k=1}^{R}(\mathcal{B}_{qi}\mathcal{K}_{ik})^T(\mathcal{B}_{qi}\mathcal{K}_{ik}) > \left(\sum_{k=1}^{R} n_{ik}(p)\mathcal{B}_{qi}\mathcal{K}_{ik}\right)^T \times \left(\sum_{k=1}^{R} n_{ik}(p)B_{qi}\mathcal{K}_{ik}\right)$$

Above eq. (53) can be rewritten as:

$$(\Lambda_g)^T(\Lambda_g) \leq p^T\left[\textstyle\sum_{k=1}^{R}(\mathcal{B}_{qi}\mathcal{K}_{ik})^T(\mathcal{B}_{qi}\mathcal{K}_{ik})\right]p \tag{54}$$

Thus, by substituting eq. (52) and eq. (54) in eq. (51), we obtain

$$\begin{aligned}\mathcal{A}\{\mathcal{V}(p,i)\} &\leq p^T\Big\{\textstyle\sum_{j=1}^{R} n_{ij}^2(p)\left[\left(\mathcal{G}_{ij} - \tfrac{1}{2}\pi_i\mathbf{I}\right)\mathcal{P}_i + \mathcal{P}_i\left(\mathcal{G}_{ij} - \tfrac{1}{2}\pi_i\mathbf{I}\right)\right] + 2\textstyle\sum_{j<k}^{R} n_{ij}(p)n_{jk}(p) \\ &\quad \left[\left(\mathcal{H}_{ijk} - \tfrac{1}{2}\pi_i\mathbf{I}\right)^T\mathcal{P}_i + \mathcal{P}_i\left(\mathcal{H}_{ijk} - \tfrac{1}{2}\pi_i\mathbf{I}\right)\right] + \textstyle\sum_{l=1;l\neq i}^{N}\pi_{il}\mathcal{P}_l + (\mathcal{A}_{qi}^T\mathcal{A}_{qi}) \\ &\quad +2\mathcal{P}_i\mathcal{P}_i + \textstyle\sum_{v=1}^{R}(\mathcal{B}_{qi}\mathcal{K}_{iv})^T(\mathcal{B}_{qi}\mathcal{K}_{iv})\Big\}p\end{aligned} \tag{55}$$

Now, multiplying eq. (43) by $n_{ij}^2(p)$ and eq. (45) by $2n_{ij}(p)n_{ik}(p)$, we have

$$\begin{array}{l}\sum_{j=1}^{R} n_{ij}^2(p)\left[\left(\mathcal{G}_{ij}-\frac{1}{2}\pi_i\mathbf{I}\right)^T\mathcal{P}_i+\mathcal{P}_i\left(\mathcal{G}_{ij}-\frac{1}{2}\pi_i\mathbf{I}\right)\right]\\ +\sum_{j=1}^{R} n_{ij}^2(p)\left[\sum_{l=1;l\neq i}^{N}\pi_{il}P_l+\mathcal{A}_{qi}^T\mathcal{A}_{qi}+2\mathcal{P}_i\mathcal{P}_i+\sum_{v=1}^{R}(\mathcal{B}_{qi}\mathcal{K}_{iv})^T(\mathcal{B}_{qi}\mathcal{K}_{iv})\right]<0\end{array} \tag{56}$$

and

$$\begin{array}{l}2\sum_{j<k}^{R} n_{ij}(p)n_{jk}(p)\left[\left(\mathcal{H}_{ijk}-\frac{1}{2}\pi_i\mathbf{I}\right)^T\mathcal{P}_i+\mathcal{P}_i\left(\mathcal{H}_{ijk}-\frac{1}{2}\pi_i\mathbf{I}\right)\right]\\ +2\sum_{j<k}^{R} n_{ij}(p)n_{jk}(p)\times\left[\sum_{l=1;l\neq i}^{N}\pi_{il}\mathcal{P}_l+\mathcal{A}_{qi}^T\mathcal{A}_{qi}+2\mathcal{P}_i\mathcal{P}_i+\sum_{v=1}^{R}(\mathcal{B}_{qi}\mathcal{K}_{iv})^T(\mathcal{B}_{qi}\mathcal{K}_{iv})\right]<0\end{array} \tag{57}$$

Adding eq. (56) to eq. (57) and using eq. (36), then:

$$\sum_{j=1}^{R} n_{ij}(p)=1$$

We get $\mathcal{A}\{\mathcal{V}(p,i)\}<0$ for $p\neq 0$.
Now, defining

$$\begin{array}{rcl}\mathbb{L}(\bar{\mathcal{G}}_{ij},\bar{\mathcal{H}}_{ijk},\mathcal{P}_i) &:=& (\bar{\mathcal{G}}_{ij}^T\mathcal{P}_i+\mathcal{P}_i\bar{\mathcal{G}}_{ij})+(\bar{\mathcal{H}}_{ijk}^T\mathcal{P}_i+\mathcal{P}_i\bar{\mathcal{H}}_{ijk})\\ &+& \sum_{l=1}^{N}\pi_{il}P_i+\mathcal{A}_{qi}^T\mathcal{A}_{qi}+\sum_{v=1}^{R}(\mathcal{B}_{qi}\mathcal{K}_{iv})^T(\mathcal{B}_{qi}\mathcal{K}_{iv})+2\mathcal{P}_i\mathcal{P}_i\end{array} \tag{58}$$

with definitions:

$$\begin{array}{rcl}\bar{\mathcal{G}}_{ij} &=& \sum_{j=1}^{R} n_{ij}^2(p)\mathcal{G}_{ij}\\ \bar{\mathcal{H}}_{ijk} &=& 2\sum_{j<k}^{R} n_{ij}(p)n_{jk}(p)\mathcal{H}_{ijk}\end{array}$$

Then, substituting eq. (57) in eq. (54), we can write

$$\mathcal{A}\{\mathcal{V}(p,i)\}<p^T\mathbb{L}(\bar{\mathcal{G}}_{ij},\bar{\mathcal{H}}_{ijk},\mathcal{P}_i)p \tag{59}$$

Therefore, for all $p\neq 0$ and $i\in\mathbf{S}$, we have

$$\frac{\mathcal{A}\{\mathcal{V}(p,i)\}}{V(p,i)} < \frac{p^T\mathbb{L}(\bar{\mathcal{G}}_{ij},\bar{\mathcal{H}}_{ijk},\mathcal{P}_i)p}{p^T\mathcal{P}_ip}\leq-\rho \tag{60}$$

where ρ is a positive constant given by:

$$\|T_\zeta^\omega\|_\infty=sup_{\omega\in\mathcal{L}_2[0,T]}\frac{\mathcal{E}\|\zeta\|_2}{\|\omega\|_2} \tag{61}$$

Implementing Dynkin's formula [40], we get:

$$\mathcal{E}\left[\mathcal{V}(p(t),r(t))\right]-\mathcal{V}(p_0,r_0)=\mathcal{E}\left[\int_0^t\mathcal{A}\{\mathcal{V}(p(\alpha),r(\alpha))\}d\alpha\right] \tag{62}$$

Then, substituting eq. (60) in eq.(62), we obtain

$$\begin{array}{rcl}\mathcal{E}\left[\mathcal{V}(p(t),r(t))\right] &\leq& \mathcal{E}\left[\int_0^t-\rho\mathcal{V}(p(\alpha),r(\alpha))d\alpha\right]\\ &=& -\rho\int_0^t\mathcal{E}\left[\mathcal{V}(p(\alpha),r(\alpha))d\alpha\right]\end{array} \tag{63}$$

Using the Gronwall–Bellman Lemma in eq. (63), we have

$$\mathcal{E}\left[\mathcal{V}(p(t),r(t))\right]\leq\mathcal{V}(p_0,r_0)e^{-\rho t} \tag{64}$$

By integrating both sides of eq. (64) with limit as $\mathcal{T}\to\infty$, it results

$$\lim_{\mathcal{T}\to\infty}\mathcal{E}\left[\int_0^{\mathcal{T}}(p^T\mathcal{P}_ip)dt|p_0,r_0\right]\leq\frac{1}{\rho}\lambda_{\max}[\mathcal{P}_i]p_0^Tp_0 \tag{65}$$

Considering the fact that in eq. (65) $\mathcal{P}_i=\mathcal{P}_i^T$, $\mathcal{P}_i>0$ for all $i\in\mathbf{S}$, the result follows by Definition 1. □

Remark 3 *The Lyapunov function plays an imperative role in stability analysis. The designer should keep all the parameters of the desired plant in mind when creating the Lyapunov function. Researchers tended to design the Lyapunov function in various ways, e.g., the direct method, the Barbashin–Krasovskii method, and LaSalle's Invariance Principle. Each Lyapunov function has its own benefits and limitations. In the case of the direct method, for example, we have no control over the plants. With the same consequences, if we use the Barbashin–Krasovskii method, and LaSalle's Invariance Principle, it creates some conservatism. On the other hand, to reduce these kinds of problems, efficient Lemmas need to be introduced. In this research, the authors studied fuzzy control design using both a two-level structured fuzzy model and fuzzy model approximation error between fuzzy models and nonlinear systems. It is actually possible for nonlinear control systems to suffer from deteriorated stability and performance due to approximation error. We then developed a systematic approach for developing robust fuzzy control using a coupled Lyapunov function and stochastic stability that assures the closed-loop gain is less than or equal to a prescribed value in the presence of bounded disturbances. In comparison with that of [40], this proposed algorithm has an efficient computational burden. In the near future, we as the authors should investigate such kind of problem with a mode-dependent Lyapunov function as in [40]. In this way, we as the authors believe that this kind of function contains more information about the plant and will deliver an excellent result in the stability analysis.*

Theorem 2 *For the given system,* MPFS *(38) with p_0 and r_0 are the initial conditions, and then our closed–loop system is stochastically stabilized with the fuzzy control law (34), and has the H_∞ performance index for all admissible uncertainties, if there exists matrices $\mathcal{P}_i = \mathcal{P}_i^T$, $\mathcal{P}_i > 0$ of proper dimensions satisfying:*

$$\sum_{l=1;l\neq i}^{N} \pi_{il} P_l + \mathcal{A}_{qi}^T \mathcal{A}_{qi} + \left(\mathcal{G}_{ij} - \frac{1}{2}\pi_i \boldsymbol{I}\right)^T \mathcal{P}_i + \mathcal{P}_i \left(\mathcal{G}_{ij} - \frac{1}{2}\pi_i \boldsymbol{I}\right)$$
$$+ \sum_{v=1}^{R} (B_{pi}K_{iv})^T (B_{pi}K_{iv}) + \left(2 + \frac{1}{\gamma^2}\right) \mathcal{P}_i \mathcal{P}_i + \mathcal{S}_i < 0; \quad j = 1, \cdots, R \tag{66}$$

$$\sum_{l=1;l\neq i}^{N} \pi_{il} P_l + \mathcal{A}_{qi}^T \mathcal{A}_{qi} + \left(\mathcal{H}_{ijk} - \frac{1}{2}\pi_i \boldsymbol{I}\right)^T \mathcal{P}_i + \mathcal{P}_i \left(\mathcal{H}_{ijk} - \frac{1}{2}\pi_i \boldsymbol{I}\right)$$
$$+ \sum_{v=1}^{R} (\mathcal{B}_{qi}\mathcal{K}_{iv})^T (\mathcal{B}_{qi}\mathcal{K}_{iv}) + \left(2 + \frac{1}{\gamma^2}\right) \mathcal{P}_i \mathcal{P}_i + \mathcal{S}_i < 0; \quad j < k; \quad j,k = 1, \cdots, R \tag{67}$$

for all $i \in \mathbf{S}$

Proof: Now, we proceed the proof with the mode at time t be i, that is $r = i, i \in \mathbf{S}$ and assume the closed–loop MPFS (38) when $\omega \neq 0$. Select the Lyapunov function as in (46), substituting (38) in (48), and proceeding in a similar way as in the proof of Theorem 1, we obtain:

$$\begin{aligned} \mathcal{A}\{\mathcal{V}(p,i)\} \;\leq\; & p^T \Big\{ \textstyle\sum_{j=1}^{R} n_{ij}^2(p) \left[\left(\mathcal{G}_{ij} - \tfrac{1}{2}\pi_i \mathbf{I}\right) \mathcal{P}_i + \mathcal{P}_i \left(\mathcal{G}_{ij} - \tfrac{1}{2}\pi_i \mathbf{I}\right) \right] + 2 \textstyle\sum_{j<k}^{R} n_{ij}(p) n_{jk}(p) \\ & \left[\left(\mathcal{H}_{ijk} - \tfrac{1}{2}\pi_i \mathbf{I}\right)^T \mathcal{P}_i + \mathcal{P}_i \left(H_{ijk} - \tfrac{1}{2}\pi_i \mathbf{I}\right) \right] + \textstyle\sum_{l=1;l\neq i}^{N} \pi_{il} \mathcal{P}_i + (\mathcal{A}_{qi}^T \mathcal{A}_{qi}) \\ & + 2P_i P_i + \textstyle\sum_{v=1}^{R} (B_{pi}K_{iv})^T (B_{pi}K_{iv}) \Big\} p + p^T \mathcal{P}_i \omega + p \mathcal{P}_i \omega^T \end{aligned} \tag{68}$$

Inequality (68) can be written as shown in (69):

$$\begin{aligned}
\mathcal{A}\{\mathcal{V}(p,i)\} &< p^T\Big\{\sum_{j=1}^{R} n_{ij}^2(p)\left[\left(\mathcal{G}_{ij}-\tfrac{1}{2}\pi_i\mathbf{I}\right)\mathcal{P}_i+\mathcal{P}_i\left(\mathcal{G}_{ij}-\tfrac{1}{2}\pi_i\mathbf{I}\right)\right]+2\sum_{j<k}^{R} n_{ij}(p)n_{jk}(p)\\
&\quad\left[\left(\mathcal{H}_{ijk}-\tfrac{1}{2}\pi_i\mathbf{I}\right)^T\mathcal{P}_i+\mathcal{P}_i\left(\mathcal{H}_{ijk}-\tfrac{1}{2}\pi_i\mathbf{I}\right)\right]+\sum_{l=1;l\neq i}^{N}\pi_{il}P_i+(\mathcal{A}_{qi}^T\mathcal{A}_{qi})\\
&\quad+2\mathcal{P}_i\mathcal{P}_i+\sum_{v=1}^{R}(\mathcal{B}_{qi}\mathcal{K}_{iv})^T(\mathcal{B}_{qi}\mathcal{K}_{iv})\Big\}p\\
&\quad+\left(p^T\mathcal{P}_i\omega+p\mathcal{P}_i\omega^T-\gamma^2\omega^T\omega-\tfrac{1}{\gamma^2}p^T\mathcal{P}_i\mathcal{P}_ip\right)+\gamma^2\omega^T\omega+\tfrac{1}{\gamma^2}p^T\mathcal{P}_i\mathcal{P}_ip\\
&= p^T\Big\{\sum_{j=1}^{R} n_{ij}^2(p)\left[\left(\mathcal{G}_{ij}-\tfrac{1}{2}\pi_i\mathbf{I}\right)\mathcal{P}_i+\mathcal{P}_i\left(\mathcal{G}_{ij}-\tfrac{1}{2}\pi_i\mathbf{I}\right)\right]+2\sum_{j<k}^{R} n_{ij}(p)n_{jk}(p)\\
&\quad\left[\left(\mathcal{H}_{ijk}-\tfrac{1}{2}\pi_i\mathbf{I}\right)^T\mathcal{P}_i+\mathcal{P}_i\left(\mathcal{H}_{ijk}-\tfrac{1}{2}\pi_i\mathbf{I}\right)\right]+\sum_{l=1;l\neq i}^{N}\pi_{il}\mathcal{P}_i+(\mathcal{A}_{qi}^T\mathcal{A}_{qi})\\
&\quad+\sum_{v=1}^{R}(B_{pi}K_{iv})^T(B_{pi}K_{iv})+2P_iP_i\Big\}p\\
&\quad-\left(\tfrac{1}{\gamma}\mathcal{P}_ip-\gamma\omega\right)^T\left(\tfrac{1}{\gamma}\mathcal{P}_ip-\gamma\omega\right)+\gamma^2\omega^T\omega+\tfrac{1}{\gamma^2}p^T\mathcal{P}_i\mathcal{P}_ip\\
&< p^T\Big\{\sum_{j=1}^{R} n_{ij}^2(p)\left[\left(\mathcal{G}_{ij}-\tfrac{1}{2}\pi_i\mathbf{I}\right)\mathcal{P}_i+\mathcal{P}_i\left(\mathcal{G}_{ij}-\tfrac{1}{2}\pi_i\mathbf{I}\right)\right]+2\sum_{j<k}^{R} n_{ij}(p)n_{jk}(p)\\
&\quad\left[\left(\mathcal{H}_{ijk}-\tfrac{1}{2}\pi_i\mathbf{I}\right)^T\mathcal{P}_i+\mathcal{P}_i\left(\mathcal{H}_{ijk}-\tfrac{1}{2}\pi_i\mathbf{I}\right)\right]+\sum_{l=1;l\neq i}^{N}\pi_{il}\mathcal{P}_i+(\mathcal{A}_{qi}^T\mathcal{A}_{qi})\\
&\quad+\sum_{v=1}^{R}(\mathcal{B}_{qi}\mathcal{K}_{iv})^T(\mathcal{B}_{qi}\mathcal{K}_{iv})+2\mathcal{P}_i\mathcal{P}_i\Big\}p+\gamma^2\omega^T\omega+\tfrac{1}{\gamma^2}p^T\mathcal{P}_i\mathcal{P}_ip
\end{aligned}\tag{69}$$

With the exitance of $\mathcal{P}_i=\mathcal{P}_i^T$, $\mathcal{P}_i>0$ and $i\in\mathbf{S}$, satisfying (66) and (67). Multiplying both sides of (66) by $n_{ij}^2(p)$ and both sides of (67) by $2n_{ij}(p)n_{ik}(p)$, we obtain

$$\begin{aligned}
&\sum_{j=1}^{R} n_{ij}^2(p)\left[\left(\mathcal{G}_{ij}-\tfrac{1}{2}\pi_i\mathbf{I}\right)^T\mathcal{P}_i+\mathcal{P}_i\left(\mathcal{G}_{ij}-\tfrac{1}{2}\pi_i\mathbf{I}\right)\right]\\
+\;&\sum_{j=1}^{R} n_{ij}^2(p)\left[\sum_{l=1;l\neq i}^{N}\pi_{il}P_i+\mathcal{A}_{qi}^T\mathcal{A}_{qi}+2\mathcal{P}_i\mathcal{P}_i+\sum_{v=1}^{R}(\mathcal{B}_{qi}\mathcal{K}_{iv})^T(\mathcal{B}_{qi}\mathcal{K}_{iv})\right]\\
<\;&-\sum_{j=1}^{R} n_{ij}^2(p)\left(\mathcal{S}_i+\tfrac{1}{\gamma^2}\mathcal{P}_i\mathcal{P}_i\right)
\end{aligned}\tag{70}$$

and

$$\begin{aligned}
&2\sum_{j<k}^{R} n_{ij}(p)n_{jk}(p)\left[\left(\mathcal{H}_{ijk}-\tfrac{1}{2}\pi_i\mathbf{I}\right)^T\mathcal{P}_i+\mathcal{P}_i\left(\mathcal{H}_{ijk}-\tfrac{1}{2}\pi_i\mathbf{I}\right)\right]\\
+\;&2\sum_{j<k}^{R} n_{ij}(p)n_{jk}(p)\times\left[\sum_{l=1;l\neq i}^{N}\pi_{il}\mathcal{P}_i+\mathcal{A}_{qi}^T\mathcal{A}_{qi}+2\mathcal{P}_i\mathcal{P}_i+\sum_{v=1}^{R}(\mathcal{B}_{qi}\mathcal{K}_{iv})^T(\mathcal{B}_{qi}\mathcal{K}_{iv})\right]\\
<\;&-\sum_{j<k}^{R} n_{ij}(p)n_{jk}(p)\left(\mathcal{S}_i+\tfrac{1}{\gamma^2}\mathcal{P}_i\mathcal{P}_i\right)
\end{aligned}\tag{71}$$

Now, adding (70) to (71) with the help of (36) and $\sum_{j=1}^{R} n_{ij}(p)=1$, we have

$$\begin{aligned}
&\sum_{j=1}^{R} n_{ij}^2(p)\left[\left(\mathcal{G}_{ij}-\tfrac{1}{2}\pi_i\mathbf{I}\right)^T\mathcal{P}_i+\mathcal{P}_i\left(\mathcal{G}_{ij}-\tfrac{1}{2}\pi_i\mathbf{I}\right)\right]\\
+\;&2\sum_{j<k}^{R} n_{ij}(p)n_{ik}(p)\times\left[\left(\mathcal{H}_{ijk}-\tfrac{1}{2}\pi_i\mathbf{I}\right)^T\mathcal{P}_i+\mathcal{P}_i\left(H_{ijk}-\tfrac{1}{2}\pi_i\mathbf{I}\right)\right]\\
+\;&\sum_{l=1;l\neq i}^{N}\pi_{il}P_l+\mathcal{A}_{qi}^T\mathcal{A}_{qi}+2\mathcal{P}_i\mathcal{P}_i+\sum_{v=1}^{R}(\mathcal{B}_{qi}\mathcal{K}_{iv})^T(\mathcal{B}_{qi}\mathcal{K}_{iv})\\
<\;&-\left(\mathcal{S}_i+\tfrac{1}{\gamma^2}\mathcal{P}_i\mathcal{P}_i\right)
\end{aligned}\tag{72}$$

Now, pre and post-multiplying to (72) by p^T and its transpose, we can obtain easily:

$$\begin{aligned}
\mathcal{A}\{\mathcal{V}(p,i)\} &< -p^T\left(\mathcal{S}_i+\gamma^2\omega^T\omega+\tfrac{1}{\gamma^2}\mathcal{P}_i\mathcal{P}_i\right)p+\tfrac{1}{\gamma^2}p^T\mathcal{P}_i\mathcal{P}_ip\\
&= -p^T\mathcal{S}_ip-\gamma^2\omega^T\omega
\end{aligned}\tag{73}$$

Now we consider the disturbance input $\omega\equiv 0$ in (73) we have $\mathcal{A}\{\mathcal{V}(p,i)\}<0$, which guarantees the asymptotic stability according to Theorem 1. Integrating both sides of (73), we get:

$$\mathcal{E}\left[\int_0^T\mathcal{A}\mathcal{V}(p(t),r(t))dt\right]+\mathcal{E}\left[\int_0^T p(\alpha)^T\mathcal{S}_ip(\alpha)d\alpha\right]-\gamma^2\int_0^T\omega(t)^T\omega(t)dt<0\tag{74}$$

Finally, putting the values (62) in (74) gives

$$\mathcal{E}\left[\mathcal{V}(p(T),r(T))\right]-\mathcal{V}(p_0,r_0)<-\mathcal{E}\left[\int_0^T p(t)^T\mathcal{S}_ip(t)dt\right]+\gamma^2\int_0^T\omega(t)^T\omega(t)dt\tag{75}$$

In the same consequences, after getting the *LMIs*, inequalities (66) and (67) are written as:

$$\begin{aligned}
&\mathcal{A}_{ij}^T\mathcal{P}_i+\mathcal{P}_i\mathcal{A}_{ij}-\mathcal{K}_{ij}^T\mathcal{B}_{ij}^T\mathcal{P}_i-\mathcal{P}_i\mathcal{B}_{ij}\mathcal{K}_{ij}-\pi_i\mathcal{P}_i\\
&+\sum_{l=1;l\neq i}^{N}\pi_{il}\mathcal{P}_l+\mathcal{A}_{qi}^T\mathcal{A}_{qi}+\sum_{v=1}^{R}(\mathcal{B}_{qi}\mathcal{K}_{iv})^T(\mathcal{B}_{qi}\mathcal{K}_{iv})\\
&+\left(2+\frac{1}{\gamma^2}\right)\mathcal{P}_i\mathcal{P}_i+\mathcal{S}_i<0;\quad j=1,\cdots,R
\end{aligned}\tag{76}$$

and

$$\begin{aligned}
&\mathcal{A}_{ij}^T\mathcal{P}_i + \mathcal{P}_i\mathcal{A}_{ij} - \mathcal{K}_{ik}^T\mathcal{B}_{ij}^T\mathcal{P}_i - \mathcal{P}_i\mathcal{B}_{ij}\mathcal{K}_{ik} + \mathcal{A}_{ik}^T\mathcal{P}_i + \mathcal{P}_i\mathcal{A}_{ik} - \mathcal{K}_{ij}^T\mathcal{B}_{ik}^T\mathcal{P}_i - \mathcal{P}_i\mathcal{B}_{ik}\mathcal{K}_{ij} - \pi_i\mathcal{P}_i \\
&+ \sum_{l=1;l\neq i}^{N}\pi_{il}\mathcal{P}_l + \mathcal{A}_{qi}^T\mathcal{A}_{qi} + \sum_{v=1}^{R}(\mathcal{B}_{qi}\mathcal{K}_{iv})^T(\mathcal{B}_{qi}\mathcal{K}_{iv}) + \left(2+\frac{1}{\gamma^2}\right)\mathcal{P}_i\mathcal{P}_i + \mathcal{S}_i < 0; \\
&j<k; \quad j,k=1,\cdots,R
\end{aligned} \tag{77}$$

Now, we multiplied by the Pre– and post–multiplying (76) and (77) by $\mathcal{P}_i^{-1}$, we get:

$$\begin{aligned}
&\mathcal{X}_i\mathcal{A}_{ij}^T + \mathcal{A}_{ij}\mathcal{X}_i - \mathcal{Y}_{ij}^T\mathcal{B}_{ij}^T - \mathcal{B}_{ij}\mathcal{Y}_{ij} - \pi_i\mathcal{X}_i + \sum_{l=1;l\neq i}^{N}\pi_{il}(\mathcal{X}_i\mathcal{X}_l^{-1}\mathcal{X}_i) + \left(2+\frac{1}{\gamma^2}\right)\mathbf{I} \\
&+ \ \mathcal{X}_i(\mathcal{S}_i + \mathcal{A}_{qi}^T\mathcal{A}_{qi})\mathcal{X}_i + \sum_{v=1}^{R}\mathcal{Y}_{iv}^T\mathcal{B}_{qi}^T\mathcal{B}_{qi}\mathcal{Y}_{iv} < 0; \quad j=1,\cdots,R
\end{aligned} \tag{78}$$

and

$$\begin{aligned}
&\mathcal{X}_i\mathcal{A}_{ij}^T + \mathcal{A}_{ij}\mathcal{X}_i - \mathcal{Y}_{ik}^T\mathcal{B}_{ij}^T - \mathcal{B}_{ij}\mathcal{Y}_{ik} + \mathcal{X}_i\mathcal{A}_{ik}^T + \mathcal{A}_{ik}\mathcal{X}_i - \mathcal{Y}_{ij}^T\mathcal{B}_{ik}^T - \mathcal{B}_{ik}\mathcal{Y}_{ij} \\
&- \ \pi_i\mathcal{X}_i + \sum_{l=1;l\neq i}^{N}\pi_{il}(\mathcal{X}_i\mathcal{X}_l^{-1}\mathcal{X}_i) + \left(2+\frac{1}{\gamma^2}\right)\mathbf{I} + \mathcal{X}_i(\mathcal{S}_i + \mathcal{A}_{qi}^T\mathcal{A}_{qi})\mathcal{X}_i \\
&+ \ \sum_{v=1}^{R}\mathcal{Y}_{iv}^T\mathcal{B}_{qi}^T\mathcal{B}_{qi}\mathcal{Y}_{iv} < 0; \quad j<k; \quad j,k=1,\cdots,R
\end{aligned} \tag{79}$$

where

$$\mathcal{X}_i := \mathcal{P}_i^{-1} \tag{80}$$

$$\mathcal{Y}_{ij} := \mathcal{K}_{ij}\mathcal{X}_i \tag{81}$$

Remark 4 *In comparison to traditional fuzzy system studies (see [41], and [42]), the approach proposed in this work has lower computational complexity. With the non-decomposition method, the complicated decomposition of the nonlinear terms is avoided during the stability analysis process. The Markov jump mechanism plays an important role in simplifying the design of fuzzy controllers. This work proposes a method for reducing the complexity of stability analysis and controller design, which reduces the computational burden on the system.*

Now, we define the slack matrices $\hat{\mathcal{U}}_{ijk}$, $\hat{\mathcal{T}}_{ij}$, $\mathcal{Z}_i$ and $\mathcal{W}_i$ given in (82)–(85), respectively,

$$\hat{\mathcal{U}}_{ijk} := \begin{bmatrix}
\mathcal{U}_{ijk}+2I & 1 & \mathcal{X}_i & \mathcal{B}_{qi}\mathcal{Y}_{i1} & \cdots & \mathcal{B}_{qi}\mathcal{Y}_{iR} \\
1 & -\gamma^2 I & 0 & 0 & \cdots & 0 \\
\mathcal{X}_i & 0 & -(\mathcal{S}_i+\mathcal{A}_{qi}^T\mathcal{A}_{qi})^{-1} & 0 & \cdots & 0 \\
\mathcal{B}_{qi}\mathcal{Y}_{i1}^T & 0 & 0 & -I & \cdots & 0 \\
\vdots & \vdots & \vdots & \vdots & \vdots & \vdots \\
\mathcal{B}_{qi}\mathcal{Y}_{iR}^T & 0 & 0 & 0 & \cdots & -I
\end{bmatrix} \tag{82}$$

$$\hat{\mathcal{T}}_{ij} := \begin{bmatrix}
\mathcal{T}_{ij}+2I & 1 & \mathcal{X}_i & \mathcal{B}_{qi}\mathcal{Y}_{i1} & \cdots & \mathcal{B}_{qi}\mathcal{Y}_{iR} \\
1 & -\gamma^2\mathbf{I} & 0 & 0 & \cdots & 0 \\
\mathcal{X}_i & 0 & -(\mathcal{S}_i+\mathcal{A}_{qi}^T\mathcal{A}_{qi})^{-1} & 0 & \cdots & 0 \\
\mathcal{B}_{qi}\mathcal{Y}_{i1}^T & 0 & 0 & -\mathbf{I} & \cdots & 0 \\
\vdots & \vdots & \vdots & \vdots & \vdots & \vdots \\
\mathcal{B}_{qi}\mathcal{Y}_{iR}^T & 0 & 0 & 0 & \cdots & -\mathbf{I}
\end{bmatrix} \tag{83}$$

$$\mathcal{Z}_i := \left[\pi_{i1}^{1/2}\mathcal{X}_i \ \cdots \ \pi_{ii-1}^{1/2}\mathcal{X}_i \ \pi_{ii+1}^{1/2}\mathcal{X}_i \ \cdots \ \pi_{iN}^{1/2}\mathcal{X}_i \right] \tag{84}$$

$$\mathcal{W}_i := diag\left\{ \mathcal{X}_1 \ \cdots \ \mathcal{X}_{i-1} \ \mathcal{X}_{i+1} \ \cdots \ \mathcal{X}_N \right\} \tag{85}$$

$$\mathcal{T}_{ij} := \mathcal{X}_i\mathcal{A}_{ij}^T + \mathcal{A}_{ij}\mathcal{X}_i - \mathcal{Y}_{ij}^T\mathcal{B}_{ij}^T - \mathcal{B}_{ij}\mathcal{Y}_{ij} - \pi_i\mathcal{X}_i \tag{86}$$

$$\mathcal{U}_{ijk} := \mathcal{X}_i\mathcal{A}_{ij}^T + \mathcal{A}_{ij}\mathcal{X}_i - \mathcal{Y}_{ik}^T\mathcal{B}_{ij}^T - \mathcal{B}_{ij}\mathcal{Y}_{ik} + \mathcal{X}_i\mathcal{A}_{ik}^T + \mathcal{A}_{ik}\mathcal{X}_i - \mathcal{Y}_{ij}^T\mathcal{B}_{ik}^T - \mathcal{B}_{ik}\mathcal{Y}_{ij} - \pi_i\mathcal{X}_i \tag{87}$$

with the help of Schur complements, (78) and (79) can be written as:

$$\begin{bmatrix} \hat{\mathcal{T}}_{ij} & \mathcal{Z}_i \\ \bigstar & -\mathcal{W}_i \end{bmatrix} < 0, \qquad j = 1, \cdots, R \tag{88}$$

$$\begin{bmatrix} \hat{\mathcal{U}}_{ijk} & \mathcal{Z}_i \\ \bigstar & -\mathcal{W}_i \end{bmatrix} < 0, \qquad j < k, \quad j, k = 1, \cdots, R \tag{89}$$

Using *Theorem 2* with (82) and (83), we established the optimization problem to the fuzzy stochastic control design with an H_∞ performance index. □

Remark 5 *Compared to strict-feedback systems, pure–feedback systems are considered to have a more representational form, as the state variables do not have affine characteristics that can be used as mechanical design controllers. Because the hybrid system possesses the characteristics of a pure–feedback system, it is rather easy to design a controller for it. In this regard, the proposed work has the greatest advantage. In the future, this work may be extended to sliding mode controllers [43], and networked–based security control [44].*

4 Simulation Example

This section deals with how a comparative analysis was made between the supersonic T–S fuzzy model generated at the individual operating points and the original nonlinear plant. To demonstrate the efficiency of the proposed controller based on the T–S fuzzy model (38), the original nonlinear model (not the T–S fuzzy model) was used. A fuzzy control example of *SHVs* is presented in this section, which is borrowed from the reference [46].

$$\dot{p} = \sum_{i=1}^{N} m_i(z) \left[\sum_{j=1}^{R} n_{ij}(p)(\mathcal{A}_{ij}p + \mathcal{B}_{ij}u) \right] + \omega \tag{90}$$

The control effectiveness of the system (10) with the following probability, without compromising generality:

$$\prod = \begin{bmatrix} -1.7 & 0.5 & 1.2 \\ 0.6 & -0.8 & 0.2 \\ 0.1 & 0.5 & -0.6 \end{bmatrix}, \qquad \mu = \begin{bmatrix} 0.25 & 0.35 & 0.40 \end{bmatrix} \tag{91}$$

In addition, $\delta = 35.6^\circ \pm 20\%$ and $\mathcal{S}_1 = \mathcal{S}_2 = \mathcal{S}_3 = diag\begin{bmatrix} 35 & 0.15 & 0.0009 & 0.0009 & -0.1500 & 0.2789 \end{bmatrix}$, with the representation of two local linear representations (R=2) can be calculated at the point $\bar{p}$:

- For Mode 1:

$$\bar{p}_{R=1} = \begin{bmatrix} 0.485 & -0.55 & 1.149 & 1.867 & 0.405 & 0.564 \end{bmatrix}$$
$$\bar{p}_{R=2} = \begin{bmatrix} 0.730 & -0.65 & 1.065 & 1.694 & 0.330 & 0.761 \end{bmatrix}$$

- For Mode 2:

$$\bar{p}_{R=1} = \begin{bmatrix} 0.486 & -0.65 & 1.150 & 1.870 & 0.410 & 0.566 \end{bmatrix}$$
$$\bar{p}_{R=2} = \begin{bmatrix} 0.735 & -0.75 & 1.075 & 1.695 & 0.345 & 0.785 \end{bmatrix}$$

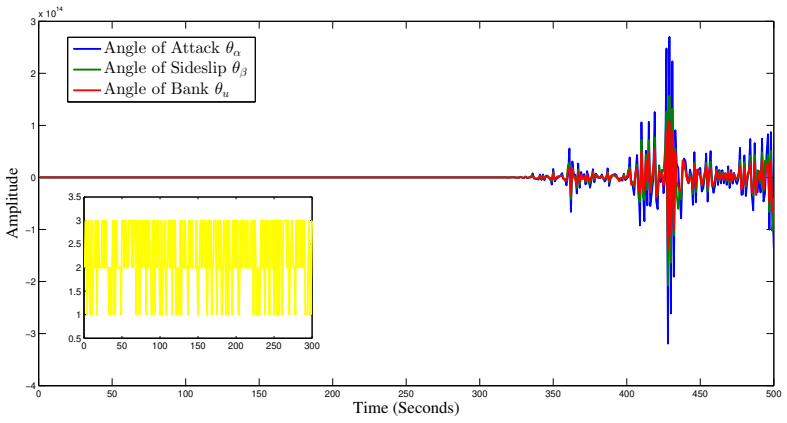

Figure 2: State trajectories of attack angle, sideslip angle, and bank angle with open–loop.

- For Mode 3:

$$\bar{p}_{R=1} = \begin{bmatrix} 0.486 & -0.70 & 1.160 & 1.880 & 0.425 & 0.575 \end{bmatrix}$$
$$\bar{p}_{R=2} = \begin{bmatrix} 0.745 & -0.90 & 1.095 & 1.767 & 0.474 & 0.832 \end{bmatrix}$$

gives the following matrices $\mathcal{A}_{ij}$, $i = 1, 2, 3$, $j = 1, 2$ for the mechanical plant. The numerical values for the physical system (38) are:

Remark 6 *During the simulation analysis, we primarily focused on stochastic types of results in order to conduct the control analysis. The Markov jump system has many practical applications such as transportation, energy, manufacturing, and communications. In addition, we as authors attempted to capture the high nonlinear dynamics of the plant, introducing Markov processes in the form of jumping modes. The problem we studied required such an analysis, so we examined it. Additionally, H_∞ control has played an influential role in different types of non-controllers, e.g., what will happen without active response or apparent behavior; it is for this reason that these analyses are a part of the research.*

Mode 1:

$$\mathcal{A}_{11} = \begin{bmatrix} 0 & 0.17453 & 0 & 0 & 1 & 0 \\ -0.17453 & 0 & 0 & 0 & 0 & -1 \\ 0.17453 & 0 & 0 & -1 & 0 & 0 \\ 0 & 0 & 0 & 0 & 1253.5 & 0 \\ 0 & 0 & 0 & 0.011223 & 0 & -0.17222 \\ 0 & 0 & 0 & 0 & 332.21 & 0 \end{bmatrix}, \quad \mathcal{B}_{11} = \begin{bmatrix} 0 \\ 0 \\ 0 \\ 31.983 \\ 0 \\ 8.4714 \end{bmatrix}$$

$$\mathcal{A}_{12} = \begin{bmatrix} 0 & 0.17453 & 0 & 0 & 1 & 0 \\ -0.17453 & 0 & 0 & 0 & 0 & -1 \\ 0 & 0 & 0 & -1 & 0 & 0 \\ 0 & 0 & 0 & 0 & -451.69 & 0 \\ 0 & 0 & 0 & 0.04586 & 0 & -0.16099 \\ 0 & 0 & 0 & 0 & -119.48 & 0 \end{bmatrix}, \quad \mathcal{B}_{12} = \begin{bmatrix} -0.1 \\ 0 \\ 0.13583 \\ 0 \\ -1 \\ 0 \end{bmatrix}$$

Mode 2:

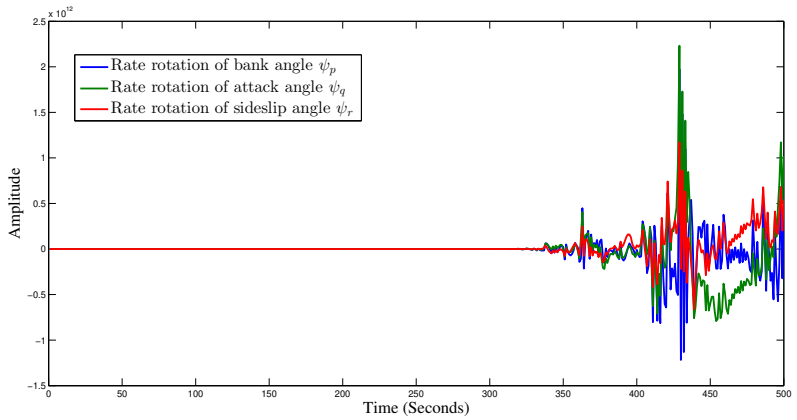

Figure 3: State trajectories of the rate of rotation of bank angle, sideslip angle, and attack angle with open–loop.

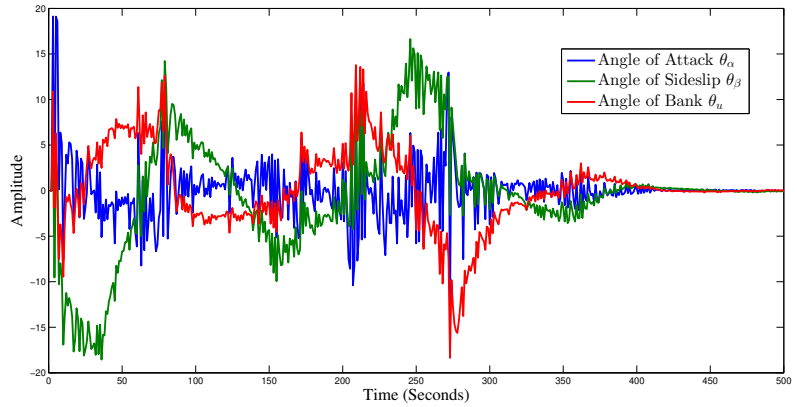

Figure 4: State trajectories of attack angle, sideslip angle, and bank angle with closed–loop.

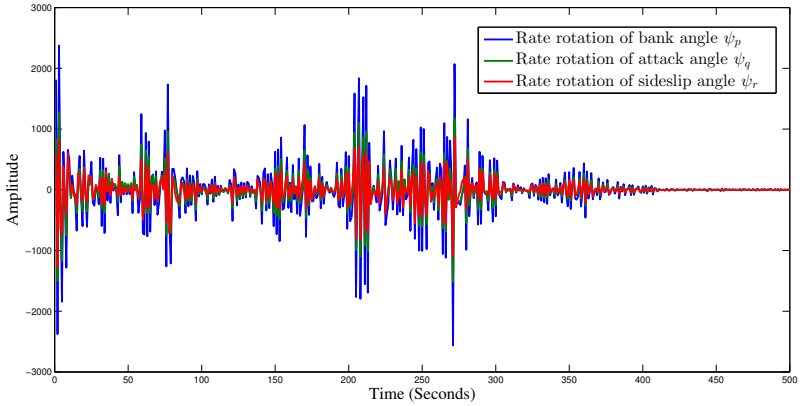

Figure 5: State trajectories of the rate of rotation of bank angle, sideslip angle, and attack angle with closed–loop.

$$\mathcal{A}_{21} = \begin{bmatrix} 0 & 0.17453 & 0 & 0 & 1 & 0 \\ -0.17453 & 0 & 0 & 0 & 0 & -1 \\ -0.17453 & 0 & 0 & -1 & 0 & 0 \\ 0 & 0 & 0 & 0 & -2156.9 & 0 \\ 0 & 0 & 0 & 0.17222 & 0 & 0.0112232 \\ 0 & 0 & 0 & 0 & -571.17 & 0 \end{bmatrix}, \quad \mathcal{B}_{21} = \begin{bmatrix} 0 \\ 0 \\ 0 \\ 0 \\ 0.0002 \\ 0 \end{bmatrix}$$

$$\mathcal{A}_{22} = \begin{bmatrix} 0 & 0 & 0 & 0 & 1 & 0 \\ 0 & 0 & 0 & 0 & 0 & -1 \\ 0.17453 & 0 & 0 & -1 & 0 & 0 \\ 0 & 0 & 0 & 0 & 1705.2 & 0 \\ 0 & 0 & 0 & -0.16099 & 0 & -0.04586 \\ 0 & 0 & 0 & 0 & 451.69 & 0 \end{bmatrix}, \quad \mathcal{B}_{22} = \begin{bmatrix} 0 \\ 0 \\ 0 \\ 0 \\ -0.0045 \\ 0 \end{bmatrix}$$

Mode 3:

$$\mathcal{A}_{31} = \begin{bmatrix} 0 & -0.17453 & 0 & 0 & 1 & 0 \\ 0.17453 & 0 & 0 & 0 & 0 & -1 \\ 0.17453 & 0 & 0 & -1 & 0 & 0 \\ 0 & 0 & 0 & 0 & 2156.9 & 0 \\ 0 & 0 & 0 & -0.17222 & 0 & -0.0112232 \\ 0 & 0 & 0 & 0 & 571.17 & 0 \end{bmatrix}, \quad \mathcal{B}_{31} = \begin{bmatrix} 0 \\ 0 \\ 0 \\ 8.4714 \\ 2.244 \\ 0 \end{bmatrix}$$

$$\mathcal{A}_{32} = \begin{bmatrix} 0 & -0.17453 & 0 & 1 & 0 & 0 \\ 0.17453 & 0 & 0 & 0 & 0 & -1 \\ -0.17453 & 0 & 0 & -1 & 0 & 0 \\ 0 & 0 & 0 & 0 & -1253.5 & 0 \\ 0 & 0 & 0 & -0.011223 & 0 & 0.17222 \\ 0 & 0 & 0 & 0 & -332.21 & 0 \end{bmatrix}, \quad \mathcal{B}_{32} = \begin{bmatrix} 0 \\ 0 \\ 0 \\ 8.4654 \\ 2.184 \\ 0 \end{bmatrix}$$

Let's assume the initial conditions $p_0 = \begin{bmatrix} 1 \\ -3 \\ 5 \\ -7 \\ 8.5 \\ -6 \end{bmatrix}$, and implementing the algorithm (see Table 1), which is a modified Algorithm adopted by [45]. The following performance is considered for the stability of the mechanical system. With the value of $\gamma = 6.45$, it observed that the LMIs (66)–(67) are feasible and the feasible solutions to those LMIs are obtained as follows:

$$\mathcal{K}_{11} = \begin{bmatrix} -0.0007 & -0.0002 & 0.0007 & 0.0002 & -0.0130 & -0.0000 \\ 0.0422 & -0.0514 & 0.0788 & -0.0023 & 0.0000 & 0.0009 \\ -0.0002 & 0.0002 & -0.0002 & 0.0001 & 0.0005 & 0.0000 \end{bmatrix}$$

$$\mathcal{K}_{12} = \begin{bmatrix} -0.0560 & -0.0500 & 0.0041 & 0.0008 & -0.0007 & 0 \\ 0.0022 & -0.0026 & 0.0040 & -0.0001 & 0 & 0.0130 \\ -0.2000 & 0.0030 & -0.0200 & 0.0070 & 0.0870 & 0.0002 \end{bmatrix}$$

$$\mathcal{K}_{21} = 10^{-5} \times \begin{bmatrix} -0.0088 & -0.0025 & 0.0088 & 0.0025 & -0.1631 & 0 \\ 0.5296 & -0.6450 & 0.9888 & -0.0289 & 0 & 0.0113 \\ -0.0025 & 0.0025 & -0.0025 & 0.0013 & 0.0063 & 0.0439 \end{bmatrix}$$

$$\mathcal{K}_{22} = 10^{-4} \times \begin{bmatrix} -0.0069 & -0.0020 & 0.0069 & 0.0020 & -0.1284 & 0 \\ 0.4167 & -0.5076 & 0.7781 & -0.0227 & 0 & 0.0089 \\ -0.0020 & 0.0020 & -0.0020 & 0.0010 & 0.0049 & 0.0346 \end{bmatrix}$$

$$\mathcal{K}_{31} = 10^{-4} \times \begin{bmatrix} -0.0032 & -0.0009 & 0.0032 & 0.0009 & 0.0594 & 0.0685 \\ 0.1928 & -0.2348 & 0.3599 & -0.0105 & -0.1370 & 0.0041 \\ -0.0009 & 0.0009 & -0.0009 & 0.0005 & 0.0023 & -0.0160 \end{bmatrix}$$

$$\mathcal{K}_{32} = 10^{-3} \times \begin{bmatrix} -0.0011 & -0.0003 & 0.0011 & 0.0003 & -0.0208 & -0.0240 \\ 0.0675 & -0.0822 & 0.1260 & -0.0037 & 0.0480 & 0.0014 \\ -0.0003 & -0.0003 & 0.0003 & 0.0002 & 0.0008 & 0.0056 \end{bmatrix}$$

Table 1: An algorithm for the design procedure.

Step-A	Model the system (90) as dynamics of (8)–(13), with membership functions and matrixes are based on their membership functions.
Step-B	Define the positive define matrix and γ performance index, which has given in Theorem 2 with unknown controller gain.
Step-C	Theorem 2 says that if an LMI meets the prescribed parameters, then it is feasible. To update the parameter, follow step-B if LMIs are not feasible.
Step-D	According to equation (80)–(81), Theorem 2 provides feasible solutions for constructing the controller parameters. In Matlab, we then run Simulink to obtain simulation results.

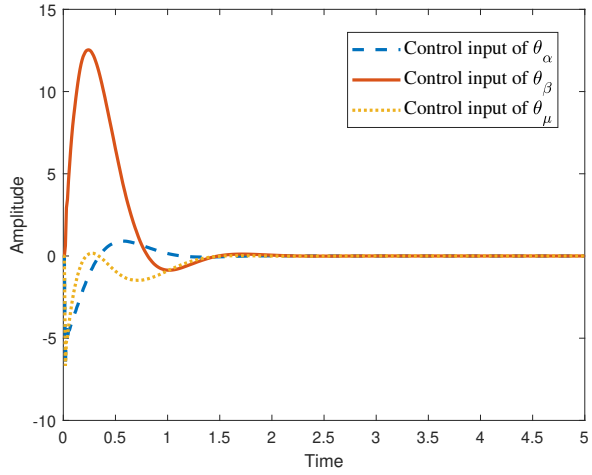

(a) Control Input without jumping modes.

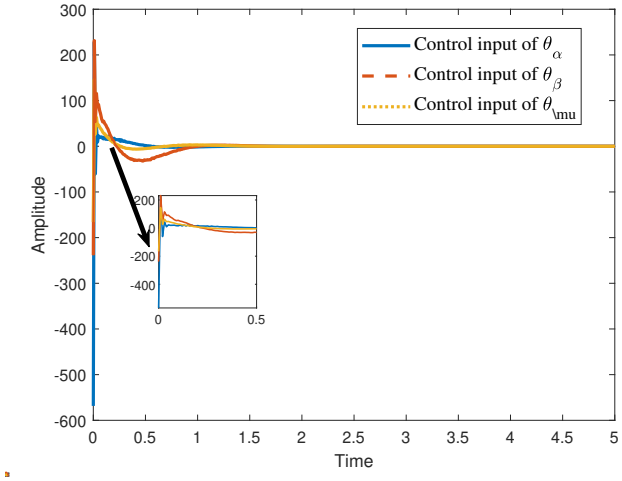

(b) Control Input with jumping modes.

Figure 6: Control inputs with and without jumping mode effects.

Then, the H_∞ control parameters can be obtained in the form of $\mathcal{Y}_{ij} = \mathcal{K}_{ij}\mathcal{X}_i$. Figures 2, 3, 4 & 5 depicted the open–loop system and closed–loop system, respectively, which reveals that the dynamics of the mechanical plant could finally approach zero. In addition, we as the authors present the jumping mode effect over the nonlinear system

in Figure 6. Furthermore, the simulations showed that the system was stable, which is necessary for investigating fuzzy neural problems.

Remark 7 *There are many dynamic systems that experience time delays, such as chemical processes, microwave oscillators, nuclear reactors, and hydraulic systems. Due to the fact that time delay can cause instability. Research studies into the stability and control issues related to time-delay systems have been conducted extensively over the past few decades. For this reason, this research attempts to develop and establish a novel Lyapunov function for a novel SHV model. Hence, stability analysis and controller design problems were addressed using the Lyapunov functional method. LMIs are linear matrix inequalities derived from the results. However, there are no acceptable methods of incorporating time delays into nonlinear systems. Because of its slow-variant time behavior, determining the exact time delay is rather difficult in practice. With new reliable time–delay assumptions, we as the authors should take this effect into account further in the future. Meanwhile, stochastic systems have been successfully used to describe mechanical systems in order to represent such load changes. The dynamics of highly nonlinear systems were taken into account during our research. Stochastic systems appear to be the best tool in this scenario.*

4.1 Robustness Analysis

In this section, we performed robustness analysis and the robustness in the nonlinear system. For these robust control designs, we took into account the approximating errors Λ_f and Λ_g among the nonlinear system and a fuzzy system model. In this scenario, the mechanical part has the subsequent bounding matrices.

Mode 1:

$$\mathcal{A}_{q1} = \begin{bmatrix} 0 & -0.17453 & 0 & 0 & 1 & 0 \\ 0.17453 & 0 & 0 & 0 & 0 & -1 \\ 0 & 0 & 0 & -1 & 0 & 0 \\ 0 & 0 & 0 & 451.69 & 0 & 0 \\ 0 & 0 & 0 & -0.04586 & 0 & -0.16099 \\ 0 & 0 & 0 & 0 & 119.48 & 0 \end{bmatrix}$$

Mode 2 & 3:

$$\mathcal{A}_{q2} = \begin{bmatrix} 0 & 0 & 0 & 0 & 1 & 0 \\ 0 & 0 & 0 & 0 & 0 & -1 \\ 0 & 0 & 0 & -1 & 0 & 0 \\ 0 & 0 & 0 & 0 & 0 & 0 \\ 0 & 0 & 0 & 0 & 0 & 0 \\ 0 & 0 & 0 & 0 & 0 & 0 \end{bmatrix} \quad \mathcal{A}_{q3} = \begin{bmatrix} 0 & 0 & 0 & 0 & 0 & 0 \\ 0 & 0 & 0 & 0 & 0 & 0 \\ 0 & 0 & 0 & 0 & 0 & 0 \\ 0 & 0 & 0 & 0 & 1 & 0 \\ 0 & 0 & 0 & 0 & 0 & -1 \\ 0 & 0 & 0 & -1 & 0 & 0 \end{bmatrix}$$

Remark 8 *The stability of a system is mainly influenced by external disturbances. By analyzing the system, performance indicators can be determined, which can lead to a more stable system. For the standard single analysis, by adjusting weighting matrices and scalars, performance can be converted into a general performance index. So, this can enable a system analysis to be as comprehensive and general as possible.*

With the value of $\gamma = 4.50$, then it computed that the LMIs (66)–(67) were practical and the effective solutions to individual LMIs are achieved as shown:

$$\mathcal{K}_{11} = \begin{bmatrix} -0.0257 & -0.0067 & 0.0271 & 0.0087 & -0.5083 & -0.0004 \\ 1.6501 & -2.0097 & 3.0774 & -0.0886 & 0.0002 & 0.0370 \\ -0.0068 & 0.00721 & -0.0067 & 0.0023 & 0.0190 & 0.0001 \end{bmatrix}$$

$$\mathcal{K}_{12} = \begin{bmatrix} 0.0064 & 0.0017 & -0.0068 & -0.0022 & 0.1271 & 0.0001 \\ -0.4125 & 0.5024 & -0.7693 & 0.0222 & -0.0001 & -0.0092 \\ 0.0017 & -0.0018 & 0.0017 & -0.0006 & -0.0047 & -0.0150 \end{bmatrix}$$

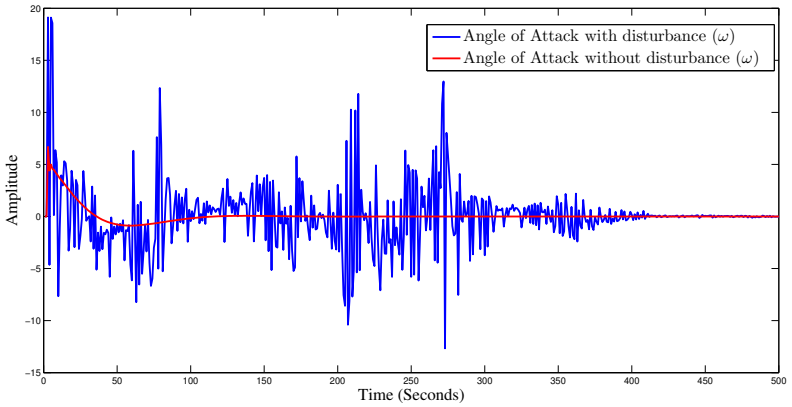

Figure 7: Performance analysis of attack angle with and without disturbance.

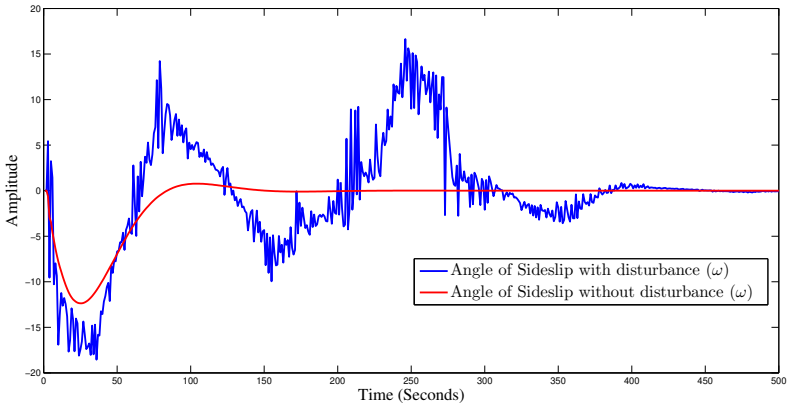

Figure 8: Performance analysis of sideslip angle with and without disturbance.

$$\mathcal{K}_{21} = \begin{bmatrix} -0.1928 & -0.0503 & 0.2032 & 0.0653 & -3.8122 & -0.0030 \\ 12.3758 & -15.0728 & 23.0805 & -0.6645 & 0.0015 & 0.2775 \\ -0.0510 & 0.0541 & -0.0503 & 0.0173 & 0.1425 & 0.0008 \end{bmatrix}$$

$$\mathcal{K}_{22} = \begin{bmatrix} 0.2249 & 0.0586 & -0.2371 & -0.0761 & 4.4476 & 0.0035 \\ -14.4384 & 17.5849 & -26.9273 & 0.7752 & -0.0018 & -0.3237 \\ 0.0595 & -0.0631 & 0.0586 & -0.0201 & -0.1663 & -0.00098 \end{bmatrix}$$

$$\mathcal{K}_{31} = \begin{bmatrix} 0.3277 & 0.0854 & -0.3455 & -0.1109 & 6.4808 & 0.0051 \\ -21.0388 & 25.6237 & -39.2368 & 1.1297 & -0.0026 & -0.4718 \\ 0.0867 & -0.0919 & 0.0854 & -0.0293 & -0.2422 & -0.0013 \end{bmatrix}$$

$$\mathcal{K}_{32} = \begin{bmatrix} -0.3570 & -0.0931 & 0.3764 & 0.1208 & -7.0603 & -0.0056 \\ 22.9199 & -27.9147 & 42.7451 & -1.2307 & 0.0028 & 0.5139 \\ -0.0945 & 0.1001 & -0.0931 & 0.0319 & 0.2639 & 0.0014 \end{bmatrix}$$

In Figures 7, 8 & 9, we focused on all angles with and without disturbance. As to the problem of *sustainable hypersonic gliding vehicles*, angles are of relatively high importance in keeping the accuracy of the destination. As can be seen from these figures, after the addition of the disturbance, our system still remained stable after some random behavior of the states. Meanwhile, we also checked the impact of force moment on the states. In Figure 10, first, we increased the value of $\mathcal{C}_{\mathcal{Y}}$ step by step for the attack angle and we observed that within the unity range, this system could keep the state in stability region. This is because if we increase the value more, the system becomes unstable. Then, we did the same analysis for the angle of sideslip and bank angle with the force moment $\mathcal{C}_{\mathcal{L}}$ and $\mathcal{C}_{\ell}$ in Figures 11 and 12. According to the above-made, our proposed algorithm could be considered to successfully

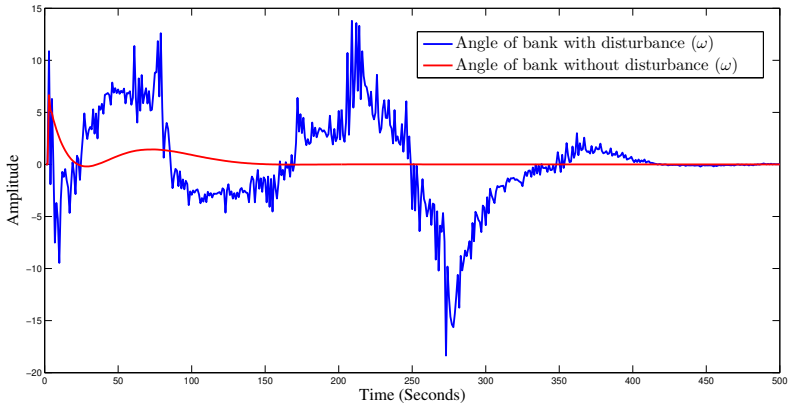

Figure 9: Performance analysis of bank angle with and without disturbance.

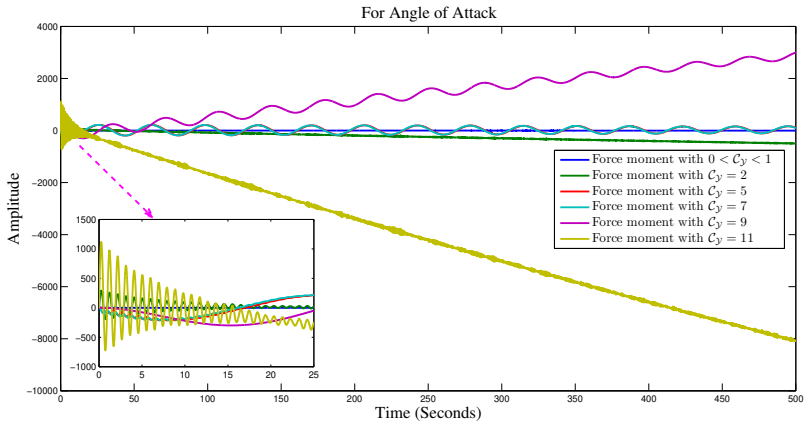

Figure 10: Robustness analysis for attack angle with different values of force moment $\mathcal{C}_{\mathcal{Y}}$.

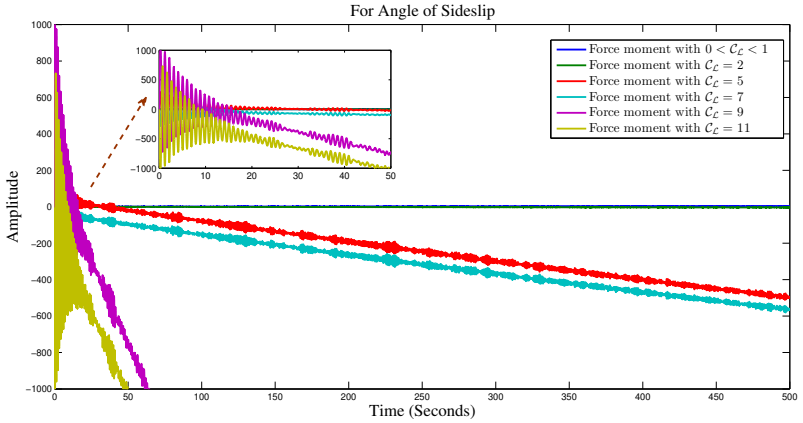

Figure 11: Robustness analysis for sideslip angle with different values of force moment $\mathcal{C}_{\mathcal{L}}$.

address the problem accuracy and track issues.

Remark 9 *In the optimization method, computational complexity is very significant. The computational complexity depends upon the number of unknown variables. These types of variables are usually defined in the Theorem, which is used to calculate the controller gains (if a control problem), filter parameters (if a problem is related to filter design), etc. In addition, if the problem also involves a Markov jump process, then computational complexity is significantly affected by the number of modes. In the proposed method, if the researcher introduces more positive definite matrixes,*

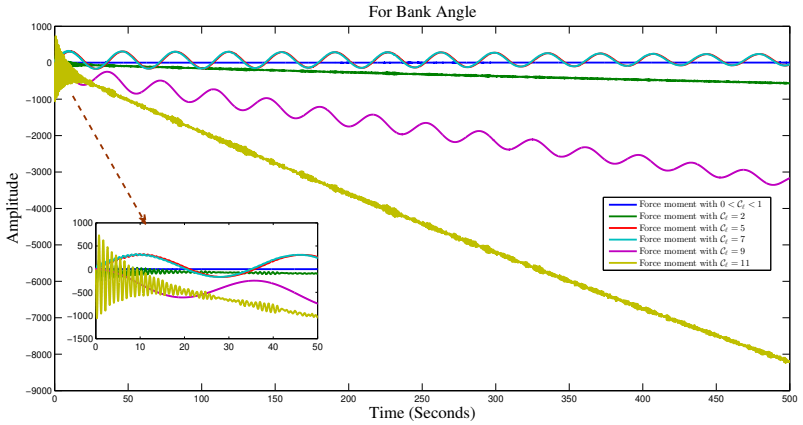

Figure 12: Robustness analysis for bank angle with different values of force moment $\mathcal{C}_\ell$.

then computational complexity will increase. On the other hand, the computational complexity mainly relies upon the size of the matrix, running time, and memory demand of the algorithm to calculate the matrix. Table 2 compares disturbance attenuation levels γ by different methods for various π_{11}. According to Theorem 2, the designed controller in (80)-(81) achieves better results at the minimum attenuation level than those in [49] and [50].

Table 2: A comparison of the minimum allowed γ.

π_{11}	0.5	1.6	2.4	3.5	4
[49]	4.545	4.452	4.390	4.315	4.284
[50]	2.436	4.124	4.108	4.091	4.019
Theorem 2	1.867	1.614	1.432	1.113	1.008

5 Conclusions

In this research, an investigation into the issues of fuzzy modeling with H_∞ fuzzy control in the *SHV* re-entry dynamics system was conducted. After the affine nonlinear system was established using appropriate hypotheses, the stochastic T–S fuzzy model to the *SHV* re-entry dynamics system was built using Taylor's expansion and fuzzy linearization procedures. It is proved that the suggested method can be integrated with the realistic control design in nonlinear systems with external disturbances, so it could be handled powerfully using convex optimization methods. Also, this fuzzy–model–based control design based on *LMI* has the advantage of allowing us to examine a more refined characterization of the nonlinear system's parameter variances. The proposed technique is considered to be useful in simulations when it comes to the stabilization of mechanical systems.

Conflicts of interest

There are no conflicts of interest between the authors.

Availability of data and material

Upon request, the corresponding author can provide the data used to develop the findings of this work.

Informed Consent

Not Applicable.

Ethics approval

The authors have not performed any animal studies for this article.

Acknowledgement

A Ph.D. fund *20z14* was used to fund this research.

References

[1] S. Türk, M. Deveci, E. Özcanzcan, F. Canitez, & R. John. Interval Type-2 Fuzzy Sets Improved by Simulated Annealing for Locating the Electric Charging Stations, *Information Sciences*, vol. 547, pp: 641–666, 2020.

[2] J. Zhu, X. Wang, H. Zhang. Six sigma robust designoptimization for thermal protection system of hypersonic vehicles based on successive response surface method, *Chinese Journal of Aeronautics*, vol. 32, no. 9, pp: 2095–108, 2019.

[3] Y. Yi, L. Xu, H. Shen, X. Fan. Disturbance observer–based L_1 robust tracking control for hypersonic vehicles with T–S disturbance modeling, *International Journal of Advanced Robotic Systems*, vol. 13, pp: 1–10, 2016.

[4] F. Chen, L. Hu, C. Wen. Improved adaptive fault–tolerant control design for hypersonic vehicle based on interval type–2 T-S model, *International Journal of Robust and Nonlinear Control*, vol. 28, no. 3, pp: 1097–1115, 2018.

[5] X. Yin, X. Li, L. Liu, Y. Wan, X. Wei. A probabilistic robust mixed H_2/H_∞ fuzzy control method for hypersonic vehicles based on reliability theory, *International Journal of Advanced Robotic Systems*, vol. 15, no. 1, 2018.

[6] X. Hu, C. Guo, C. Hu, B. He. Sliding mode learning control for T–S fuzzy system and an application to hypersonic flight vehicle, *Asian Journal of Control*, doi:10.1002/asjc.2822, 2022.

[7] Z. Preitl, R.E. Precup, J.K. Tar, M. Takăcs. Use of multi-parametric quadratic programming in fuzzy control systems, *Acta Polytechnica Hungarica*, vol. 3, no. 3, pp: 29–43, 2006.

[8] X. Ping and W. Pedrycz. Output Feedback Model Predictive Control of Interval Type–2 T–S Fuzzy System With Bounded Disturbance, *IEEE Transactions on Fuzzy Systems*, vol. 28, no. 1, pp: 148–162, 2020.

[9] S. Liang, B. Xu, J. Ren. Kalman-filter-based robust control for hypersonic flight vehicle with measurement noises, *Aerospace Science and Technology*, vol. 112, 106566, 2021.

[10] S. Daneshvar Dehnavi, C. Negri, S. Bayne, M. Giesselmann. Dynamic Voltage Restorer (DVR) with a novel robust control strategy, *ISA transactions*, vol. 121, pp: 316–26, 2022.

[11] S.A. Ardjoun, M. Denaï, H. Chafouk. A Robust Control Approach for Frequency Support Capability of Grid–Tie Photovoltaic Systems, *Journal of Solar Energy Engineering*, vol. 145, no. 2, 021009, 2022.

[12] L. Ovalle, H. Ríos, H. Ahmed. Robust control for an active suspension system via continuous sliding-mode controllers, *Engineering Science and Technology, an International Journal*, vol. 28, 101026, 2022.

[13] R. Merco, F. Ferrante, R.G. Sanfelice, P. Pisu. Robust output feedback control design in the presence of sporadic measurements, *IEEE Transactions on Automatic Control*, DOI: 10.1109/TAC.2022.3213616, 2022.

[14] S. Ullah, Q. Khan, A. Mehmood, S.A. Kirmani, O. Mechali. Neuro-adaptive fast integral terminal sliding mode control design with variable gain robust exact differentiator for under-actuated quadcopter UAV, *ISA transactions*, Vol. 120, pp: 293–304, 2022.

[15] M.T. Vu, K.A. Alattas, Y. Bouteraa, R. Rahmani, A. Fekih, S. Mobayen, W. Assawinchaichote. Optimized Fuzzy Enhanced Robust Control Design for a Stewart Parallel Robot, *Mathematics*, vol. 10, no. 11, 1917, 2022.

[16] G. Zhuang, X. Wang, J. Xia, Y. Wang. Observer-based asynchronous feedback H_∞ control for delayed fuzzy implicit jump systems under HMM and event–trigger mechanisms, *Information Sciences*, vol. 631, pp: 45–64, 2023.

[17] X. Li, D. Ye, D., Membership–function–dependent security control for networked T–S fuzzy–model–based systems against DoS attacks, *IET Control Theory & Applications*, 2021.

[18] M. S. Aslam, P. Tiwari, H. M. Pandey and S. S. Band. Observer–Based Control for a New Stochastic Maximum Power Point tracking for Photovoltaic Systems With Networked Control System, *IEEE Transactions on Fuzzy Systems*, pp: 1–14, doi: 10.1109/TFUZZ.2022.3215797, 2022.

[19] Claudia-Adina Bojan-Dragos, R.E. Precup, S. Preitl, R.C. Roman, E.L. Hedrea, A.I. Szedlak–Stinean. GWO–Based Optimal Tuning of Type–1 and Type–2 Fuzzy Controllers for Electromagnetic Actuated Clutch Systems, *IFAC–PapersOnLine*, vol. 54, no. 4, pp: 189–194, 2021.

[20] R. He, L. Liu, G. Tang, W. Bao, Entry trajectory generation without reversal of bank angle, *Aerospace Science and Technology*, vol. 71, pp: 627–635, 2017,

[21] Y. Xu, Z. Wang, D. Y. Yao, R. Q. Lu, C. Y. Su. State estimation for periodic neural networks with uncertain weight matrices and markovian jump channel states, *IEEE Transactions on Systems, Man, and Cybernetics: Systems*, vol. 48, no. 11, pp: 1841–1850, 2018.

[22] J. Li, Q. Zhang, X. Yan. Integral sliding mode control for Markovian jump T–S fuzzy descriptor systems based on the super–twisting algorithm, *IET Control Theory & Application*, vol. 11, no. 8, pp: 1134–1143, 2017.

[23] X. Xiao, J.H. Park, L. Zhou. New results on stability analysis of Markovian switching singular systems, *IEEE Transactions on Automic Control*, vol. 64, no. 5, pp: 2084–2091, 2019.

[24] Y. Yin, P. Shi, F. Liu, K. L. Teo and C. Lim. J. Cheng, J.H. Park, M. Chadli. Peak–to–peak fuzzy filtering of nonlinear discrete–time systems with markov communication protocol, *Information Sciences*, Vol. 607, pp: 361–376, 2022.

[25] Y. Fei, P. Shi, C. P. Lim and X. Yuan. Finite–Time Observer–Based Formation Tracking With Application to Omni-Directional Robots, *IEEE Transactions on Industrial Electronics*, pp:1–9, doi: 10.1109/TIE.2022.3224186, 2022.

[26] L.X. Zhang, Z.P. Ning, P. Shi. Input–output approach to control forfuzzy Markov jump systems with time–varying delays and uncertainpacket dropout rate, *IEEE Transactions on Cybernitics*, vol. 45, no. 11, pp: 2449–2460, 2015.

[27] H. Shen, Y. Z. Men, Z. G. Wu, J. H. Park. Nonfragile H_∞ control for fuzzy markovian jump systems under fast sampling singular perturbation, *IEEE Transactions on Systems, Man and Cybernetics: Systems*, vol. 48, no. 12, pp: 2058–2069, 2018.

[28] J. Tao, R. Q. Lu, P. Shi, H. Y. Su, Z. G. Wu. Dissipativity–basedreliable control for fuzzy Markov jump systems with actuator faults, *IEEE Transactions on Cybernitics*, vol. 47, no. 9, pp: 2377–2388, 2017.

[29] B. Yao, M. Tomizuka. Adaptive robust control of siso nonlinear systems in a semi-strict feedback form, *Automatica*, vol. 33, no. 5, pp: 893–900, 1997.

[30] J. Wang, Y. Gao, Y. Liu, J. Liu, G. Sun, L. Wu. Intelligent dynamic practical–sliding–mode control for singular Markovian jump systems, *Information Sciences*, vol. 607, pp:153–172, 2022.

[31] P. Shi, H. Wang, C.C. Lim. Network–Based Event–Triggered Control for Singular Systems With Quantizations, *IEEE Transactions on Industrial Electronics*, vol. 63, no. 2, pp: 1230–1238, 2016.

[32] J. Bai, R. Lu, H. Su, A. Xue. Modeling and H_∞ control of wireless networked control system with both delay and packet loss, *Journal of the Franklin Institute*, vol. 352, no. 10, pp: 3915–3928, 2015.

[33] P. Cheng, M. Chen, V. Stojanovic, S. He. Asynchronous fault detection filtering for piecewise homogenous Markov jump linear systems via a dual hidden Markov model, *Mechanical Systems and Signal Processing*, vol. 151, 107353, 2021.

[34] P.K. Singh, A. Pljonkin, L. Zhou. Modeling and PID control of quadrotor UAV based on machine learning, *Journal of Intelligent Systems*, doi.org/10.1515/jisys-2021-0213, 2022.

[35] K.e. Shao, J. Zheng, H. Wang, F. Xu, X. Wang, B. Liang. Recursive sliding mode control with adaptive disturbance observer for a linear motor positioner, *Mechanical Systems and Signal Processing*. vol. 146, 107014, 2021.

[36] X. Du , X. Sun , Z. Wang , A. Dai. A scheduling scheme of linear model predictive controllers for turbofan engines, *IEEE Access*, vol. 5, pp: 24533–24541, 2017.

[37] B. Yang , X. Wang , P. Sun. Non–affine parameter dependent LPV model and LMI based adaptive control for turbofan engines, *China Journal of Aeronautics*, vol. 32, no. 3, pp: 585–594, 2019.

[38] M. Pan , K. Zhang , Y. Chen , J. Huang. A new robust tracking control design for turbofan engines: H_∞/leitmann approach, *Applied Sciences*, vol. 7, no. 5, pp: 1–21, 2017.

[39] Y. Y. Cao and J. Lam. Robust H_∂ control of uncertain Markovian jump systems with time–delay, *IEEE Transactions on Automic Control*, vol. 45, no. 1, pp: 77–83, 2000.

[40] B. Zhang, W. X. Zheng and S. Xu. Filtering of Markovian Jump Delay Systems Based on a New Performance Index, *IEEE Transactions on Circuits and Systems I: Regular Papers*, vol. 60, no. 5, pp: 1250–1263, 2013.

[41] W.I. Lee, B.Y. Park, S.H. Kim. Relaxed observer–based stabilization and dissipativity conditions of T–S fuzzy systems with nonhomogeneous Markov jumps via non–PDC scheme, *Applied Mathematics and Computation*, vol. 434, 27455, 2022.

[42] B. Visakamoorthi, K. Subramanian, P. Muthukumar. Hidden Markov model based non–fragile sampled–data control design for mode–dependent fuzzy systems with actuator faults, *Applied Mathematics and Computation*, vol. 435, 127454, 2022.

[43] C. Zhang, D. Gong, Q. Gao, W. Chen, J. Wang. A fuzzy integral sliding–mode parallel control approach for nonlinear descriptor systems, *Information Sciences*, vol. 615, pp: 491–503, 2022.

[44] Z. Ning, T. Wang, K. Zhang. Dynamic event–triggered security control and fault detection for nonlinear systems with quantization and deception attack, *Information Sciences*, vol. 594, pp: 43–59, 2022.

[45] M.S. Aslam, Z. Chen. Observer–based dissipative output feedback control for network T–S fuzzy systems under time delays with mismatch premise, *Nonlinear Dynamics*, vol. 95, pp: 2923–2941, 2019.

[46] W. Zhang, X. Huang, and X.Z. Gao. T–S Fuzzy Modelling and Attitude Control for Hypersonic Gliding Vehicles, *Mathematical Problems in Engineering*, vol. 2017, Article ID: 6574527, pages: 14, https://doi.org/10.1155/2017/6574527, 2017.

[47] B. Zhang, W. X. Zheng and S. Xu. Filtering of Markovian Jump Delay Systems Based on a New Performance Index, *IEEE Transactions on Circuits and Systems I: Regular Papers*, vol. 60, no. 5, pp: 1250–1263, 2013.

[48] M. Li, J. Zhao, J. Xia, G. Zhuang, W. Zhang. Extended dissipative analysis and synthesis for network control systems with an event–triggered scheme, *Neurocomputing*, vol. 312, pp: 34–40, 2018.

[49] L. Li, Q. Zhang, B. Zhu. H_∞ fuzzy control for nonlinear time–delay singular markovian jump systems with partly unknown transition rates, *Fuzzy Sets and Systems*, vol. 254, pp: 106–125, 2014.

[50] J. Ren, G. He, J. Fu. Robust H_∞ sliding mode control for nonlinear stochastic T–S fuzzy singular Markovian jump systems with time–varying delays, *Information Sciences*, vol. 535, pp: 42–63, 2020.